Chapter

Molecular Mechanisms and Targets of Cyclic Guanosine Monophosphate (cGMP) in Vascular Smooth Muscles

Aleš Fajmut

Abstract

Molecular mechanisms and targets of cyclic guanosine monophosphate (cGMP) accounting for vascular smooth muscles (VSM) contractility are reviewed. Mathematical models of five published mechanisms are presented, and four novel mechanisms are proposed. cGMP, which is primarily produced by the nitric oxide (NO) dependent soluble guanylate cyclase (sGC), activates cGMP-dependent protein kinase (PKG). The NO/cGMP/PKG signaling pathway targets are the mechanisms that regulate cytosolic calcium ($[Ca^{2+}]_i$) signaling and those implicated in the Ca^{2+}-desensitization of the contractile apparatus. In addition to previous mathematical models of cGMP-mediated molecular mechanisms targeting $[Ca^{2+}]_i$ regulation, such as large-conductance Ca^{2+}-activated K^+ channels (BKCa), Ca^{2+}-dependent Cl^- channels (ClCa), Na^+/Ca^{2+} exchanger (NCX), $Na^+/K^+/Cl^-$ cotransport (NKCC), and Na^+/K^+-ATPase (NKA), other four novel mechanisms are proposed here based on the existing but perhaps overlooked experimental results. These are the effects of cGMP on the sarco−/endo- plasmic reticulum Ca^{2+}-ATPase (SERCA), the plasma membrane Ca^{2+}-ATPase (PMCA), the inositol 1,4,5-trisphosphate (IP_3) receptor channels type 1 (IP_3R1), and on the myosin light chain phosphatase (MLCP), which is implicated in the Ca^{2+}-desensitization. Different modeling approaches are presented and discussed, and novel model descriptions are proposed.

Keywords: vascular smooth muscle, contraction, relaxation, nitric oxide, cyclic guanosine monophosphate, protein kinase G, Ca^{2+} signaling, desensitization, mathematical model, ionic fluxes

1. Introduction

Cyclic guanosine 3′,5′-monophosphate (cGMP) is an intracellular second-messenger that mediates a broad spectrum of physiologic processes in multiple cell types within the cardiovascular, gastrointestinal, urinary, reproductive, nervous, endocrine, and immune systems. In particular, cGMP signaling plays a vital role in the endothelium, vascular smooth muscle cells (VSMC), and cardiac myocytes. cGMP was first synthesized in 1960, and soon after, its endogenous production was detected in rats. In the late 70s, two separate experiments confirmed that the gas nitric oxide (NO) stimulated cGMP production by activating soluble guanylate

cyclase (sGC). In 1980, it was reported that a diffusible substance causing vasodilatation is released from the endothelium. The so-called endothelium-derived relaxing factor (EDRF) was identified seven years later as NO. See [1] for review.

The molecular mechanisms of cardiovascular NO signaling are not entirely understood. Still, it is currently accepted that many effects are mediated, at least in part, via cGMP-dependent pathways. Within the cardiovascular system, these signaling pathways play a vital role in vasodilatation as well as in proliferation, migration, differentiation, and inflammation of VSMC and endothelial cells (ECs), in the modulation of myocyte contractility as well as of cardiac remodeling and thrombosis [2–4]. Impaired functioning at any signaling step from the synthesis through the effector activation and the degradation process of either NO or cGMP accounts for numerous cardiovascular diseases, such as hypertension, atherosclerosis, cardiac hypertrophy, and heart failure [3, 4]. Hence, these signaling pathways represent the potential targets for pharmacological treatment.

2. Nitric oxide (NO) and cyclic guanosine monophosphate (cGMP) production and degradation

Various stimuli can trigger relaxation responses of VSMC via the production and signaling of NO in the vascular endothelium. These are endogenous neurotransmitters (e.g., substance P and acetylcholine), humoral substances (e.g., bradykinin), and mechanical stimuli (e.g., the increase in hemodynamic shear stress or intraluminal pressure). They all trigger a complex cascade of biochemical reactions, accounting for either the mobilization, activation, or increase in the catalytic activity of NOS to produce NO or for upregulation of its gene expression. In the cardiovascular system, most of NO is produced in the endothelium by the endothelial NOS (eNOS). eNOS is also detected in cardiac myocytes, platelets, certain neurons, and kidney tubular epithelial cells. The other two isoforms are neuronal- and inducible- NOS (nNOS and iNOS, respectively). The former is mainly located in the nervous system, and the latter, which is induced by cytokines, is predominantly found in the immune system. They all catalyze the oxidation of the amino acid L-arginine into L-citrulline, where the by-product is NO [5].

Sensing of shear stress is still under intensive research since it is mediated by rapid and almost simultaneous activation of various membrane molecules and microdomains, including ion channels, tyrosine kinase receptors, G-protein-coupled receptors, caveolae, adhesion proteins, cytoskeleton, glycocalyx, primary cilia, and filaments [6]. Though the underlying biochemical signaling processes are not entirely understood, three main mechanisms of mechanotransduction were proposed. The first one involves the mechanisms which account for the entry of Ca^{2+} across the EC plasma membrane either via capacitive Ca^{2+} entry (CCE) [7] or via activation of mechanosensing ion channels (MSICs) [8]. Both processes lead to further increases in $[Ca^{2+}]_i$, its consequent interaction with calmodulin (CaM), and finally to NOS activation. The other two mechanisms cross-correlate many signaling pathways mediated by G protein-coupled receptors (GPCR) and integrins involving protein kinases A, B, C, and G (PKA, Akt, PKC, and PKG, respectively), as well as phosphatidylinositide 3-kinase (PI3K). These signaling pathways regulate the activation of different nuclear factors affecting NOS gene expression [9], the recruitment of NOS from caveolae, the phosphorylation of NOS, and the cytosolic $[Ca^{2+}]_i$ concentration and signaling [6].

Downstream the NO production cGMP is produced either by the soluble or the membrane-bound particulate guanylate cyclases, sGC and pGC, respectively, in response to either elevated NO or brain and atrial natriuretic peptides (BNP and

ANP, respectively). Natriuretic peptides (NPs) activate pGC, while NO diffuses into the cytosol, binds to, and activates sGC. cGMP exerts its action predominantly through binding and activating its target, cGMP-dependent protein kinase (PKG) [3]. There are two other types of cGMP-target effector molecules. The first type is phosphodiesterases (PDEs), which also degrade other cyclic nucleotides. The second type is nonselective cation channels, which are present in the visual and olfactory systems. PDEs degrade cGMP and, hence shape its spatiotemporal levels. CGMP also cross-regulates cyclic adenosine monophosphate levels (cAMP) since other PDEs (e.g. PDE2) that degrade both cAMP and cGMP are stimulated by cGMP [10]. In addition to PDE5, which selectively degrades cGMP, several other PDE isoforms can hydrolyze both, cGMP and cAMP. These are PDE1, PDE2, and PDE3. The strategy of inhibiting PDEs to enhance cGMP and related signaling has already been successfully used with the PDE5 inhibitors, especially sildenafil, to treat erectile dysfunction, pulmonary hypertension, and chronic heart failure [10]. Other cGMP-elevating drugs, such as nitrovasodilators that donate NO, and various NP analogs, have also been successfully used in humans to treat cardiovascular diseases. NO-generating drugs such as glyceryl trinitrate or sodium nitroprusside have been used to treat angina pectoris in humans for more than 100 years [11].

3. Calcium-contraction coupling in vascular smooth muscle cells (VSMC)

The contractile state of VSMCs is regulated dynamically by hormones and neurotransmitters via the increase of the cytosolic calcium concentration ($[Ca^{2+}]_i$). Ca^{2+} is mostly released from its intracellular store sarcoplasmic reticulum (SR) via IP_3 sensitive or ryanodine receptor channels (IP_3R and RyR, respectively). In part, Ca^{2+} entry to the cytosol could be ascribed to the fluxes across the plasma membrane via the Ca^{2+}- selective voltage-dependent channels. The rise in $[Ca^{2+}]_i$ initiates binding of Ca^{2+} to CaM and the consequent interactions of myosin light chain kinase (MLCK) with Ca^{2+}/CaM complexes. Active MLCK is the one that is bound with the Ca_4CaM complex. Active MLCK phosphorylates the regulatory myosin light chain (MLC), enabling the attachment of myosin heads to the actin filaments and cross-bridge cycling [12]. The smooth muscle cell's contractile state is determined by the extent of MLC phosphorylation regulated by the balance of MLCK and MLC phosphatase (MLCP) activities. The latter dephosphorylates MLC. High vascular tone is maintained as long as the phosphorylation rate is higher than that of dephosphorylation. Relaxation occurs when $[Ca^{2+}]_i$ decreases, which results in the dissociation of Ca^{2+} from CaM and inactivation of MLCK. In that case, the activity of MLCP predominates the activity of MLCK, and the active actin-myosin cross-bridge cycling is not established. However, a passive latch state is possible [13]. The level of smooth muscle contractility can also be modulated at constant $[Ca^{2+}]_i$. The protein kinase C (PKC) and Rho kinase (ROCK) pathways play an essential role in regulating MLCP activity. They may cause diminished activity of MLCP and result in increased levels of phosphorylated MLC and a higher tension at a given $[Ca^{2+}]_i$. This increased contractility is called Ca^{2+} sensitization [12]. In reality, the process is much more complex since it is composed of many cross-interacting pathways with different feedbacks, nonlinear behavior of the interactions, dynamical changes of many variables – especially $[Ca^{2+}]_i$ [14]. In this complex system of interactions $[Ca^{2+}]_i$ signaling still represents a bottleneck according to its bow-tie structure of encoding and decoding [15]. cGMP/PKG signaling occurs on both – the encoding and the decoding sides and represents a predominant mechanism in regulating vasoactivity, particularly vasorelaxation. More than ten substrates being

phosphorylated *in vivo* by PKG were identified, and many of them take part in the $[Ca^{2+}]_i$ encoding and decoding processes [3, 16].

3.1 cGMP-dependent protein kinase (PKG)

The enzyme PKG belongs to the family of serine/threonine (Ser/Thr) kinases. In mammals, PKG-I and PKG-II are encoded by different genes, prkg1 and prkg2, respectively. PKG-I exists in two isoforms PKG-Iα and PKG-Iβ. PKG-I is present at high concentrations in all smooth muscles, including the uterus, vessels, intestine, and trachea. PKG-II is expressed in several brain nuclei, intestinal mucosa, kidney, adrenal cortex, chondrocytes, and lung. Only PKG-Iα and PKG-Iβ are expressed in the vascular system. See [3] for a review. All types of PKG are homodimers. Each monomer contains a regulatory and a catalytic domain. Each of the PKG regulatory domains binds two cGMP molecules allosterically with high cooperativity. The affinities of the two binding sites on each of the subunits of PKG-Iα differ by approximately tenfold. Binding sites occupied by cGMP induce significant conformation changes in the molecular structure. By that, autoinhibition of the catalytic center is released, and the basal activity is increased. Hence, the phosphorylation of serine/ threonine residues of the target proteins as well as of the autophosphorylation site is possible. All four binding sites have to be occupied with cGMP for the fully active holoenzyme PKG [17]. PKG-I mediates both receptor-triggered and depolarization-induced vasorelaxation by several mechanisms. Many of them are not entirely understood, and some of them are still unknown. In general, PKG-mediated relaxation is induced either by attenuation of $[Ca^{2+}]_i$ and/or desensitization of the contractile apparatus. The first effect is achieved by negatively affecting the "$[Ca^{2+}]_i$-on" mechanisms and by positively affecting the "$[Ca^{2+}]_i$-off" mechanisms. On the $[Ca^{2+}]_i$-decoding part, PKG's effect is concentrated mainly on the activation of the MLCP, which desensitizes the contractile apparatus to $[Ca^{2+}]_i$ [18].

3.2 "$[Ca^{2+}]_i$-on" mechanisms as targets of cGMP/PKG signaling

One of the primary targets of cGMP/PKG signaling to elevate $[Ca^{2+}]_i$ is the IP_3 receptor channel type 1 (IP_3R1) and its correlated cGMP-associated kinase substrate protein (IRAG). If IRAG is colocalized with IP_3R1 and PKG-Iβ in the presence of cGMP, it inhibits Ca^{2+} release through IP_3R1 via its phosphorylation [19]. It was shown that PKG-Iβ exclusively phosphorylated only the type 1 but not the type 2 and 3 IP_3R *in vivo* and that both, PKG and PKA, phosphorylated IP_3R1 *in vitro* in gastric smooth muscles, which resulted in diminished IP_3 and Ca^{2+}-induced Ca^{2+} release (ICICR) from the SR [20]. *In vivo* experiments on mice with mutated IRAG, which did not interact with IP_3R, showed that PKG/IRAG/ IP_3R interactions indeed decrease the receptor-triggered $[Ca^{2+}]_i$ and hence contraction [21]. In the *in vitro* experiments, it was also shown that PKG-Iβ phosphorylated IRAG but not IP_3R [22]. The same was confirmed with COS-7 transfected cells where the phosphorylation of IRAG resulted in the reduced Ca^{2+} release during concurrent activation of PKA and PKG. The effect was observed for all three IP_3R sub-types [23]. It is supposed that IRAG signaling does not modulate basal tone but might be important for blood pressure regulation under pathophysiological conditions [24].

PKG-Iα may also attenuate receptor-activated contraction via inhibition of IP_3 production mediated by GPCR signaling [25] and interfering with phospholipase C-β (PLC-β) [26]. It has been shown that the isoform PKG-Iα binds, phosphorylates, and activates the regulator of G protein signaling 2 (RGS2), which terminates

the signal transduction of the contractile agonists mediated by the Gq-coupled receptors and terminates thereby the activity of PLC [25]. It was also proposed that PKG-Iα/RGS2 pathway might inhibit hormone receptor-triggered Ca^{2+} release and vasoconstriction *in vivo* [27]. It has also been shown that PKG can directly phosphorylate PLC-β *in vitro* in cultured COS-7 cells and *in vivo* in aortic VSMC, which blocked the activation of the enzymes correlated with the G-protein subunits and attenuated agonist-induced IP_3 production and Ca^{2+} release [26].

There is also evidence that PKG may cause vasodilatation by suppressing the Ca^{2+} influx across the plasma membrane through the voltage-operated Ca^{2+} channels (VOCC). cGMP/PKG has the opposite effect as cAMP/PKA on this type of channel. The former inhibited and the latter enhanced L-type Ca^{2+} channel (LTCC) activity in rabbit portal vein myocytes [28]. On the other hand, in rat cerebral arterial VSMC, which express T-type Ca^{2+} channels (TTCC) PKA [29] and PKG [30] both had a suppressing effect on their conductance. In both cases, a rightward shift of the voltage-response curve was observed. A similar effect was observed for the nonselective transient receptor potential cationic 1/3 channels (TRPC1/3) [31]. On the other hand, the experiments on the macroscopic and single-channel Ca^{2+} currents from guinea-pig basilar artery showed that the addition of 10 μM cGMP did not affect single-channel properties, such as conductance, voltage dependence, the number of open states, and different time constants, but significantly reduced the channel availability [32].

3.3 "$[Ca^{2+}]_i$-off" mechanisms as targets of cGMP/PKG signaling

cGMP/PKG is supposed to enhance the activities of all three major Ca^{2+}-removal systems in VSMCs. The Primary $[Ca^{2+}]_i$-off mechanism is refilling the Ca^{2+} stores via sarco−/endo- plasmic reticulum Ca^{2+}-ATPase (SERCA). The increase in SERCA activity in response to cGMP was first identified in isolated SR vesicles from cardiac and smooth muscles [33]. Later it was demonstrated that NO-induced relaxation of cultured VSMC from the aorta was associated with increased PKG-dependent phospholamban (PLB) phosphorylation [34]. Using a solid-state nuclear magnetic resonance (NMR) spectroscopy, it was found that PLB binds to SERCA allosterically [35]. Moreover, the phosphorylation at Ser16 of PLB, which gradually lowers PLB interaction with SERCA, was found to increase SERCA activity [35]. In gastric SMC, cGMP-mediated Ca^{2+} uptake via SERCA was observed *in vitro* in a concentration-dependent manner [36].

Experiments on cultured aortic VSMC provided evidence that cGMP also accelerates $[Ca^{2+}]_i$ extrusion by stimulating the Na^+/ Ca^{2+} exchangers (NCX) at different Na^+ concentrations [37]. cGMP increased both forward and reversed Na^+/ Ca^{2+} exchange modes by approximately 50% after adding 500 μM of membrane-permeable cGMP analog. The $[Ca^{2+}]_i$ pumping activity gradually increased with cGMP concentration. Phosphorylation by PKG was proposed as the underlying mechanism for this effect [37].

Another cGMP/PKG-mediated $[Ca^{2+}]_i$-off mechanism is the plasma membrane Ca^{2+} ATP-ase (PMCA). The evidence was first obtained with experiments on isolated proteins [38] and experiments performed on cultured VSMC [39]. All results suggested that the phosphorylation of the PMCA by PKG was responsible for stimulating the Ca^{2+}-pumping activity, which was 2.4-fold higher after adding 500 μM of membrane-permeable cGMP analog. The leftward shift in the pumping activity vs. $[Ca^{2+}]_i$ dependence was also observed [39]. Experiment on isolated and purified PMCA from porcine aorta [40] confirmed the previous two results at much smaller cGMP concentrations.

3.4 cGMP/PKG-dependent mechanisms that indirectly affect $[Ca^{2+}]_i$

The mechanisms by which cGMP/PKG signaling interferes with $[Ca^{2+}]_i$ are primarily linked with cell-membrane depolarization/hyperpolarization. Although depolarization-induced contraction remains mostly unresolved, these mechanisms are intensively studied [41]. One of the established targets of cGMP/PKG signaling is the large-conductance Ca^{2+}-activated K^+ channel (BKCa). The modulation of BKCa by different protein kinases in different smooth muscle tissues as well as the sites and mechanisms of their action remain unresolved [42]. The activation BKCa presumably hyperpolarises the cell membrane, thereby influences the gating of voltage-operated Ca^{2+} channels and lowers $[Ca^{2+}]_i$. PKG-I is known to activate BKCa either directly by phosphorylation [43] or indirectly via protein phosphatase regulation [44]. Activation of BKCa in the presence of NO/cGMP in isolated rat afferent arterioles attenuated extracellular Ca^{2+} influx upon KCl stimulation [45]. The role and importance of BKCa in vasorelaxation were highlighted with the experiments performed on BKCa-deficient mice. Their deletion led to a relatively mild increase in blood pressure. However, it increased vascular tone in small arteries due to a complete lack of spontaneous K^+ efflux and, therefore, depolarised state of the membrane, and reduced suppression of Ca^{2+} transients in response to cGMP [46].

Another mechanism by which cGMP/PKG signaling may affect $[Ca^{2+}]_i$ influx is via Ca^{2+}-activated Cl^- channels [47]. These type of channels was observed in VSMC of mesenteric resistance arteries. Since their activation required phosphorylation, was sensitive to PKG inhibitors, and was evoked by adding PKG, it is believed that the effect of cGMP on the Cl^- current is mediated through PKG [47]. The physiological role of Ca^{2+}-activated Cl^- channels is ambiguous since their excessive activation would promote an inward Cl^- current leading to cell depolarization, activation of VOCC, increase in $[Ca^{2+}]_i$, and, hence, vasoconstriction.

Information on the effect of cGMP/PKG on Na^+/K^+ ATPase (NKA) [48] and cotransport of $Na^+/K^+/Cl^-$ (NKCC) [49] in terms of VSMC physiology is very limited and vague. However, these mechanisms have been implicated in the mathematical models [50, 51]. It was reported that cGMP might increase the activity of NKCC in vascular SMC of rat thoracic aorta by up to 3.5-fold [49]. In the canine pulmonary artery SMC, nitroprusside/cGMP-mediated relaxation was accompanied by increase NKA activity [48].

3.5 cGMP/PKG signaling targeting the Ca^{2+}-desensitization mechanisms

PKG may also cause vasodilatation by desensitizing the contractile apparatus in response to elevated $[Ca^{2+}]_i$, resulting from either MLCP activation or MLCK deactivation. Both effects lead to MLC dephosphorylation, myosin cross-bridge detachment, and relaxation even at high $[Ca^{2+}]_i$. The enzyme MLCP plays a major role in the Ca^{2+}-desensitization since it is not directly Ca^{2+}-dependent, and it embodies various possibilities for regulating its activity [52]. These different options arise from its complex structure and widespread distribution in different tissues. MLCP holoenzyme is composed of three subunits – catalytic (PP1c), regulatory (MYPT1), and a small subunit (M20/M21). It is a Ser/Thr phosphatase that belongs to the protein phosphatase type 1 (PP1) family. Active PP1c is required for its catalytic activity, while MYPT1 targets the enzyme to its substrates and also autoregulates the catalytic activity of PP1c. This autoregulation emerges because MYPT1 contains different, for its structure and activity important, phosphorylation sites. In human sequence, these phosphorylation sites are Thr696 and Thr853, which are phosphorylated by ROCK [53] and other agonist-induced kinases. There are also Ser695 and Ser852 phosphorylation sites on MYPT1, which are phosphorylated by PKA and

PKG [54]. The residues Ser695 and Thr696 as well as Ser852 and Thr853, are close within the MYPT1 sequence, and thus phosphorylation of one site prevents the phosphorylation of the neighboring site. It was proposed and also demonstrated that PKA or PKG-dependent phosphorylation of Ser695 and Ser852 prevents the phosphorylation of Thr696 and Thr853 and vice versa [12, 54, 55].

The current hypothesis is that the phosphorylation of Thr696 and Thr853 induces such structural changes in MYPT1 that these phosphorylated sites interact with the MLCP catalytic subunit PP1c [56] and is supported by the fact that MYPT1 is quite flexible at this part of the structure. Moreover, the sequences around Thr696 or Thr853 are similar to that of Ser19, where MLC is phosphorylated [57]. It is hypothesized that P-Thr696 and P-Thr853 may represent either substrate analogs to P-Ser19 of MLC or a potent autoinhibitory site docking to the PP1c catalytic subunit of MLCP [56]. In all these scenarios, the MLCP-dependent rate of MLC dephosphorylation is decreased. On the other hand, if MYPT is phosphorylated at Ser695 and Ser852 beforehand, Thr696 and Thr853 phosphorylation is blocked [54, 56].

Phosphorylation of Thr853 is a less potent inhibitor of MLCP than Thr696 [56]. It was also reported that PKA could phosphorylate all four sites, Ser695, Thr696, Ser852, Thr853, simultaneously. However, such a form of MYPT1 did not inhibit PP1c [58]. Another possibility of MLCP activity inhibition is binding the phosphorylated form of PKC-potentiated phosphatase inhibitor protein of 17 kDa (CPI-17) to the catalytic subunit PP1c. The phosphorylation increases the affinity of CPI-17 for PP1c by approximately 1000-fold, resulting in suppressed MLCP activity [59]. CPI-17 is expressed predominantly in tonic smooth muscles with slow and sustained contraction, especially in VSMC from the aorta and femoral arteries. The enzymes linked with the phosphorylation of CPI-17 are PKC, ROCK, zipper-interacting protein kinase (ZIPK), integrin-linked kinase (ILK). However, PKC and ROCK are most commonly mentioned [60]. ROCK signaling interferes with PKG and PKA signaling since PKA and PKG phosphorylate RhoA, the ROCK activator. Increased level of RhoA phosphorylation attenuates ROCK activity. In this way, PKG mediates vasorelaxation via reduced activity of ROCK and the correlated reduced inhibition of MLCP. That leads to faster MLC dephosphorylation and relaxation [61].

The role of PKC and ROCK in the stimulation-contraction coupling is still not well understood [62]. It is also possible that their role and importance in different smooth muscles is different. However, it is believed that CPI-17 phosphorylation and the corresponding inhibition of MLCP is the predominant process of the early phase of contraction. It was reported that PKC is believed to be primarily responsible for fast CPI-17 phosphorylation during the early phase of vasoconstriction, and ROCK was found responsible for slow, sustained CPI-17 phosphorylation during the sustained phase of contraction [63]. On the other hand, in the rat airways, ROCK activation and the consequent MLCP inhibition contributed to the early phase of the smooth muscles' contractile response. Whatever the agonist in that system was, the ROCK inhibitor Y27632 did not modify the basal tension. Still, it decreased the amplitude of the short duration response without altering the superimposed delayed contraction [64]. That indicates that in rat airway SMC, ROCK plays a major role in CPI-17 phosphorylation and that other kinases are responsible for Thr696 and Thr853 phosphorylation [62].

Moreover, PKG may affect MLCP activity also by the phosphorylation of telokin, which is a smooth muscle-specific protein whose sequence is identical to that of the noncatalytic terminus of MLCK. Telokin does not increase MLCP activity *per se* but acts synergistically with PKA and PKG [65]. By binding to either phosphorylated MYPT1 and/or phosphorylated MLC, telokin is supposed to facilitate the interaction between the enzyme and its substrate and de-inhibits the auto-

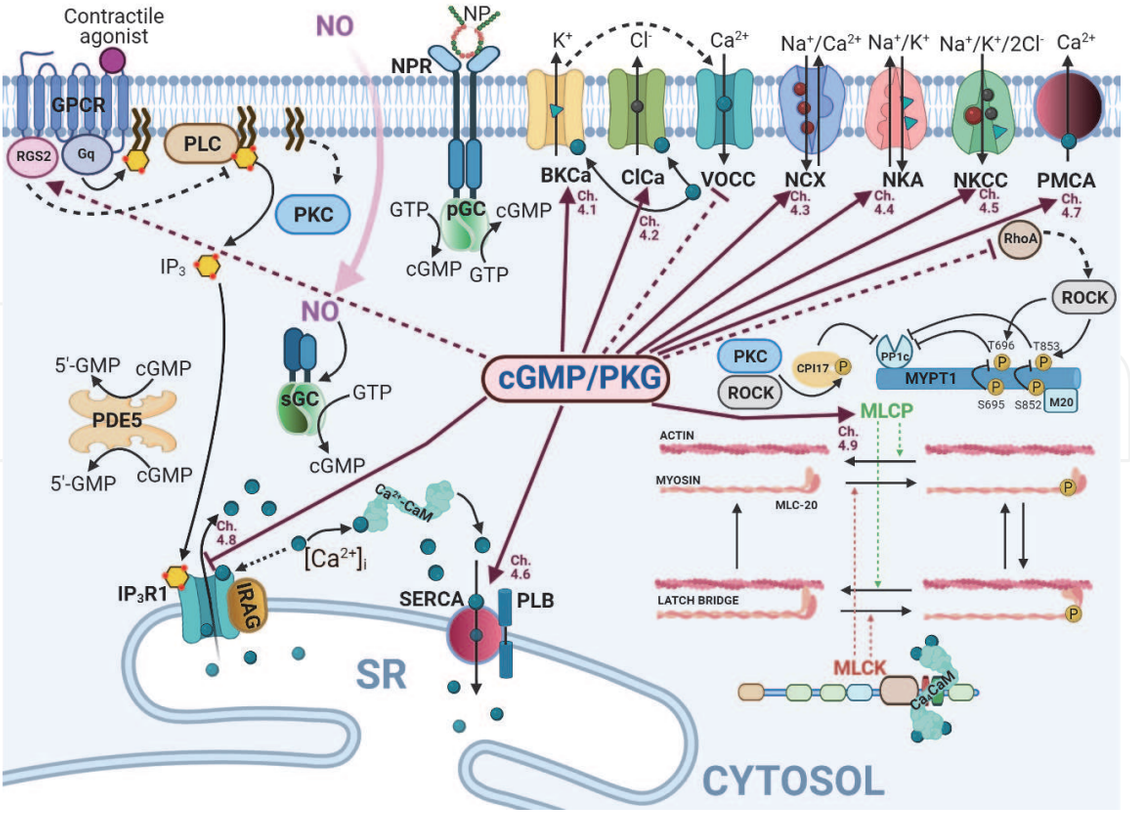

Figure 1.
Molecular mechanisms and targets of cyclic guanosine monophosphate (cGMP)/protein kinase G (PKG) signaling in vascular smooth muscle cells (VSMCs) described in chapters 4.1 to 4.9 (full dark red lines denoted with Ch. 4.1 to 4.9) and others described in the text (dashed dark red lines). For explanation see text. Abbreviations used: GPCR (G protein-coupled receptor), RGS2 (regulator of G_q protein signaling 2), G_q (G protein), PLC (phospholipase C), PKC (protein kinase C), IP_3 (inositol 1,4,5-trisphosphate), NO (nitric oxide), NPR (natriuretic peptide receptor), NP (natriuretic peptide), GTP (guanosine 5′-triphosphate), cGMP (cyclic guanosine monophosphate), 5'-GMP (guanosine 5′-monophosphate), pGC (particulate guanylate cyclase), sGC (soluble guanylate cyclase), PDE5 (phosphodiesterase 5), BKCa (large-conductance Ca^{2+}-activated K^+ channels), ClCa (Ca^{2+}-dependent Cl^- channels), VOCC (voltage-operated Ca^{2+} channel), NCX (Na^+/Ca^{2+} exchanger), NKA (Na^+/K^+-ATPase), NKCC ($Na^+/K^+/Cl^-$ cotransport), PMCA (plasma membrane Ca^{2+}-ATPase), RhoA (ROCK activator), ROCK (rho kinase), CPI-17 (PKC-potentiated phosphatase inhibitor protein of 17 kDa), PP1c (MLCP catalytic subunit), MYPT1 (MLCP regulatory subunit), M20 (MLCP small subunit), MLCP (myosin light chain phosphatase), T696/ T853 (threonine 696/853 of the MYPT1), S695/S852 (serine 696/853 of the MYPT1), MLCK (myosin light chain kinase), MLC-20 (20 kDa myosin light chain), Ca_4CaM (calmodulin with bound 4 Ca^{2+}), Ca^{2+}-CaM (Ca^{2+}-calmodulin complexes), SR (sarcoplasmic reticulum), SERCA (sarco−/endo- plasmic reticulum Ca^{2+}-ATPase), PLB (phospholamban), $[Ca^{2+}]_i$ (cytosolic Ca^{2+} concentration), IRAG (IP_3R1-correlated cGMP-associated kinase substrate protein), IP_3R1 (1,4,5-trisphosphate receptor channel type 1), P (phosphorylated form of protein).

suppressed MLCP activity emerging from Thr696 and Thr853 phosphorylation. This mechanism results in an increased rate of MLC dephosphorylation [66]. The majority of the described mechanisms and targets of cGMP/PKG signaling are summarized in **Figure 1**. 11 targets are depicted, from which 9 of them are described by mathematical models presented in the following chapter.

4. Mathematical modeling of cGMP/PKG-mediated ionic fluxes and Ca^{2+}-desensitization of the contractile apparatus

The first attempt to build a whole-cell-like model of VSMC, also considering the NO/sGC/cGMP signaling cascade, was performed by Yang et al. [67]. They upgraded their existing models for rat cerebrovascular arteries [68]. The model [67] predicted the NO-induced cGMP production and the corresponding attenuation of

$[Ca^{2+}]_i$, Ca^{2+}-desensitization of the contractile apparatus, and the reduction in force. In terms of cGMP-mediated target-regulation, they considered the effects on the BKCa and the contractile mechanism. Model simulations reproduced major NO/cGMP-induced VSMC relaxation effects. Additionally, cGMP was also considered in sGC desensitization, limiting cGMP production well below maximum [67]. The activating effect of NO/cGMP on BKCa was assumed as cGMP-dependent and partially NO-dependent.

In 2007 and 2008, another two whole-cell-like models for VSMC were presented [50, 51]. However, both focused only on $[Ca^{2+}]_i$ signaling and did not consider the processes of the contractile apparatus. Jacobsen et al. [50] focused primarily on the role of Ca^{2+}-dependent Cl^- channels that may cause the transitions between different types of $[Ca^{2+}]_i$ signals in rat mesenteric small arteries upon α-adrenoreceptor stimulation. Instead of cGMP's influence on BKCa, they considered the cGMP-dependent mechanisms of Ca^{2+}-dependent Cl^- channels and NKA. Kapela et al. [51] focused primarily on the plasma membrane electrophysiological properties and considered eleven ionic currents across the plasma membrane. Four of them considered cGMP-dependent mechanisms, i.e. Ca^{2+}-dependent Cl^- channels, BKCa, NCX, and NKCC. The model's purpose was to provide a working database of the rat mesenteric SMC physiological data. It was considered as the building block of the future multi-cellular models of the vascular wall [51].

4.1 The model of cGMP-mediated current through the large-conductance Ca^{2+}-activated K^+ channels (BKCa)

BKCa is the most frequently modeled cGMP-dependent mechanism accounting for $[Ca^{2+}]_i$ signaling. The first model of Yang et al. [67] was based on the experimental studies of Zhou et al. [69], who suggested that PKG stimulates the activity of two isoforms of BKCa either by phosphorylation of the channel or its regulatory proteins. The resultant effect on the potassium electric current (I_K) was modeled with a left-shift of the voltage dependency of equilibrium open probability ($\overline{P}_{K,o}$) towards more negative potentials [67]. The complete mathematical description of [68] follows the Hodgkin-Huxley formalism. The general expression for I_K is:

$$I_K = g_K P_{K,o}(V_m - V_K), \tag{1}$$

where g_K is a channel conductance, $P_{K,o}$ is open probability or gating of the channel and $(V_m - V_K)$ is the driving force of the current, where V_m is a membrane potential, and the V_K is the Nernst equilibrium potential. Eq. (1) is analogous to Ohm's law. The overall gating factor $P_{K,o}$ consists of two parts – a fast gating term ($P_{K,f}$) and a slow gating term ($P_{K,s}$):

$$P_{K,o} = f_K P_{K,f} + s_K P_{K,s}, \tag{2}$$

where f_K is a fraction of fast channels, and s_K is a fraction of slow channels. Fast and slow gating terms are described with a first-order ordinary differential equation for a biphasic (open-close) transition:

$$\frac{dP_{K,f}}{dt} = \frac{\overline{P}_{K,o} - P_{K,f}}{\tau_{K,f}}, \tag{3}$$

$$\frac{dP_{K,s}}{dt} = \frac{\overline{P}_{K,o} - P_{K,s}}{\tau_{K,s}}, \tag{4}$$

where $\tau_{K,f}$ and $\tau_{K,s}$ are the characteristic opening times and $\overline{P}_{K,o}$is an equilibrium open probability, which is a sigmoidal function of the membrane potential (V_m):

$$\overline{P}_{K,o} = \frac{1}{1 + e^{-\left(V_m - V_{K,1/2}\right)/S_{K,0}}}. \tag{5}$$

The parameter's value $S_{0,K}$ represents the slope of the sigmoidal function, and its sign defines the orientation (declining/ increasing). Typically, $V_{1/2,K}$ is a parameter and represents the membrane potential, at which half-maximal value $\overline{P}_{K,o}$ is achieved; however, here, it is a function of $[Ca^{2+}]_i$, $[cGMP]$, and $[NO]$:

$$V_{K,1/2} = -V_{K,Ca} \log\left(\left[Ca^{2+}\right]_i\right) - V_{K,0} - V_{K,cGMP} R_{K,cGMP} - V_{K,NO} R_{K,NO}, \tag{6}$$

where $V_{K,0}$ is a basal value of $V_{1/2}$, and $V_{K,NO}$, $V_{K,cGMP}$ and $V_{K,Ca}$ are maximal induced shifts of $V_{1/2}$ towards lower values, and, $R_{K,cGMP}$ and $R_{K,NO}$ are the regulatory Hill functions:

$$R_{K,cGMP} = \frac{[cGMP]^{n_{cGMP,K}}}{[cGMP]^{n_{cGMP,K}} + K_{cGMP,K}^{n_{cGMP,K}}}, \tag{7}$$

$$R_{K,NO} = \frac{[NO]^{n_{NO,K}}}{[NO]^{n_{NO,K}} + K_{NO,K}^{n_{NO,K}}}, \tag{8}$$

where $n_{cGMP,K}$ and $n_{NO,K}$ are the Hill coefficients and, $K_{cGMP,K}$ and $K_{NO,K}$ are the half-saturation constants. The same notation for Hill function parameters is used elsewhere in the text. The descriptions of all parameters are given in tables.

Authors Kapela et al. [51] used almost the same approach as Yang et al. [67]. In the former cas the authors used the Goldman-Hodgkin-Katz model to describe the potassium flux I_K:

$$I_K = A_m N_{BKCa} P_{K,o} P_{BKCa} V_m \frac{F^2}{RT} \frac{[K]_o - [K]_i e^{\frac{F}{RT}Vm}}{1 - e^{\frac{F}{RT}Vm}}, \tag{9}$$

where A_m is a cell-membrane surface area, N_{BKCa} is a channel density, P_{BKCa} is a single channel permeability, V_m is a membrane potential, $[K]_o$ and $[K]_i$ are the external and internal potassium concentrations, respectively, F is a Faraday constant, R is the universal gas constant, and T is the absolute temperature. These cell-specific and general parameter values could be found in [51]. cGMP-dependent gating $P_{K,o}$ is defined the same as above in Eqs. (2)–(8).

The comparison of parameter values presented in **Table 1** reveals similarities but also differences. The model of Kapela et al. [51] was written more specifically for the rat mesenteric arteriole, whereby the parameters for the BKCa were such that they fitted experimental data of [70]. In contrast, the model of Yang et al. [67] was compared with the experimental data for rabbit femoral arteries [71], and the parameters for BKca accounted for [72].

4.2 The model of cGMP-mediated current through the Ca^{2+} activated Cl^- channels (ClCa)

The model was first proposed by Jacobsen et al. [50] and was based on the measurements performed on the rat mesenteric resistance arteries [47].

Parameter	Description	Value [67]	Value [51]
g_K	Overall maximal conductance of the BKCa	0.5 nS	/
f_K	Fraction of fast channels	0.65	0.17
s_K	Fraction of slow channels	0.35	0.83
$\tau_{K,f}$	The characteristic time of fast-channel activation	0.5 ms	0.84 ms
$\tau_{K,s}$	The characteristic time of slow-channel activation	11.5 ms	35.9 ms
$S_{K,0}$	The slope of the $\overline{P}_o$ vs. V_m function	30.8 mV	18.25 mV
$V_{K,Ca}$	Maximal Ca^{2+}-induced $V_{1/2}$ shift	53.7 mV	41.7 mV
$V_{K,0}$	Basal $V_{1/2}$value	283.7 mV	128.2 mV
$V_{K,cGMP}$	Maximal cGMP-induced $V_{1/2}$ shift	66.9 mV	76 mV
$V_{K,NO}$	Maximal NO-induced $V_{1/2}$ shift	100 mV	46.3 mV
$n_{cGMP,K}$	Hill coefficient	2	2
$n_{NO,K}$	Hill coefficient	1	1
$K_{cGMP,K}$	Half saturation constant in the regulatory cGMP-dependent Hill function	0.55 μM	1.5 μM
$K_{NO,K}$	Half saturation constant in the regulatory NO-dependent Hill function	0.2 μM	0.2 μM

Table 1.
Parameter values for the cGMP-dependent Ca^{2+}-activated K^+ (BKCa) current.

The Cl^- electric current (I_{Cl}) across the plasma membrane is defined as that for potassium in Eq. (1):

$$I_{Cl} = g_{Cl} P_{Cl,o} (V_m - V_{Cl}), \tag{10}$$

The expression for $P_{Cl,o}$ is analogous to Eq. (3):

$$\frac{dP_{Cl,o}}{dt} = \frac{\overline{P}_{Cl,o} - P_{Cl,o}}{\tau_{Cl}}, \tag{11}$$

but the equilibrium open probability $\overline{P}_{Cl,o}$ is not defined according to the Hodgkin-Huxley formalism but rather with an adapted Hill-type function:

$$\overline{P}_{Cl,o} = R_{cGMP,Cl} \frac{\left[Ca^{2+}\right]_i^{n_{Ca,Cl}}}{\left[Ca^{2+}\right]_i^{n_{Ca,Cl}} + \left(K_{Ca,cGMP,Cl}(1 - \rho R_{cGMP,Cl})\right)^{n_{Ca,Cl}}}, \tag{12}$$

where $n_{Ca,Cl}$, $K_{Ca,cGMP,Cl}$ and ρ are parameters, and $R_{cGMP,Cl}$ is cGMP-dependent:

$$R_{cGMP,Cl} = \frac{[cGMP]^{n_{cGMP,Cl}}}{[cGMP]^{n_{cGMP,Cl}} + K_{cGMP,Cl}^{n_{cGMP},Cl}}. \tag{13}$$

For I_{Cl}, Kapela et al. [51] used a similar approach as Jacobsen et al. [50]. However, the former authors applied slight modifications. The general description of the Cl^- current is the same as in [50] (Eq. (10)), only the expression $P_{Cl,o}$ is different. Kapela et al. [51] considered that a fraction of Ca^{2+}-dependent Cl^- channels is cGMP dependent, and a fraction is cGMP-independent. That is evident from the two terms within the expression for $P_{Cl,o}$:

$$P_{Cl,o} = R_{I,Cl}\frac{\left[Ca^{2+}\right]_i^{n_{Ca,Cl}}}{\left[Ca^{2+}\right]_i^{n_{Ca,Cl}} + K_{Ca,Cl}^{n_{Ca,Cl}}} + R_{cGMP,Cl}\frac{\left[Ca^{2+}\right]_i^{n_{Ca,Cl}}}{\left[Ca^{2+}\right]_i^{n_{Ca,Cl}} + \left(K_{Ca,cGMP,Cl}(1-\rho R_{cGMP,Cl})\right)^{n_{Ca,Cl}}}, \quad (14)$$

where $R_{I,Cl}$ is a cGMP-independent component and $R_{cGMP,Cl}$ is defined the same as in Eq. (13). Parameter values and their descriptions are presented in **Table 2**.

The comparison of parameter values presented in **Table 2** shows remarkable similarity. However, there are two significant differences in the modeling approach. Jacobsen et al. [50], who first proposed the cGMP-dependent model for I_{Cl}, defined $P_{Cl,o}$ as a time-dependent function, whereas Kapela et al. [51] proposed an equilibrium model and omitted differential Eq. (11). On the other hand, they added a cGMP-independent term (compare Eq. (12) and Eq. (14)). In both cases, the same reference with experimental data for rat mesenteric arteries was used to determine the parameter values [47], except for the half-saturation constant in the cGMP-independent term ($K_{Ca,Cl}$) of [51], which was determined for the rat portal vein SMC [73].

It is suggested that the effect of cGMP on Ca^{2+}-activated Cl^- current is not likely to be essential for the tonic receptor-activated contractile response but rather for the synchronization among VSMCs as between VSMCs and ECs [47, 50, 74].

4.3 The model of cGMP-mediated current through the Na^+/Ca^{2+} exchanger (NCX)

The framework for the mathematical description of the plasma membrane Na^+/Ca^{2+} exchange (NCX) (I_{NCX}) in Kapela et al. was taken from the model of Di Francesco and Noble 1985 [75], which was developed for the atrial myocytes. Kapela et al. [51] adjusted the maximal exchanger conductivity, which is much lower in SMC than in atrial myocytes, and added the effect of cGMP according to the measured results of [37]:

$$I_{NCX} = I_{NCX,s}R_{NCX,cGMP}\frac{[Na^+]_i^3\left[Ca^{2+}\right]_o e^{\frac{\gamma V_m F}{RT}} - [Na^+]_o^3\left[Ca^{2+}\right]_i e^{\frac{(\gamma-1)V_m F}{RT}}}{1 + d_{NCX}\left([Na^+]_o^3\left[Ca^{2+}\right]_i - [Na^+]_i^3\left[Ca^{2+}\right]_o\right)}, \quad (15)$$

Parameter	Description	Values [50]	Values [51]
g_{Cl}	Overall maximal conductance	3.8 nS	5.75 nS
τ_{Cl}	The characteristic time constant of channel activation	50 ms	/
$n_{Ca,Cl}$	Hill coefficient	3	2
$K_{Ca,cGMP,Cl}$	Half saturation constant in cGMP-dependent factor	0.4 μM	0.4 μM
ρ	The determinant of cGMP influence on the half-saturation constant	0.9	0.9
$n_{cGMP,Cl}$	Hill coefficient	3.3	3.3
$K_{cGMP,Cl}$	Half saturation constant in the regulatory cGMP-dependent Hill function	6.4 μM	6.4 μM
$K_{Ca,Cl}$	Half saturation constant in cGMP-independent term	/	0.365 μM
$R_{I,Cl}$	Weight of the cGMP-independent term	/	0.0132

Table 2.
Parameter values for the cGMP-dependent Ca^{2+}-activated Cl^- current.

where $I_{NCX,s}$ is a scaling factor for I_{NCX}, d_{NCX} is the denominator constant, γ is voltage-dependence parameter, and $R_{NCX,cGMP}$ is a cGMP-dependent regulatory function:

$$R_{NCX,cGMP} = 1 + f_{NCX,cGMP} \frac{[cGMP]}{[cGMP] + K_{cGMP,NCX}}, \tag{16}$$

where $f_{NCX,cGMP}$ is an additional fold-increase in NCX current due to cGMP and $K_{cGMP,NCX}$ is a half-saturation constant. Parameter values are presented in **Table 3**.

In experiments [37], $[Ca^{2+}]_i$ pumping activity gradually increased with cGMP concentration. However, a 50% increase in Na^+/ Ca^{2+} exchange was observed after adding a large, probably unphysiological concentration (500 μM) of membrane-permeable cGMP analog. Hence, the effects of low cGMP concentrations on the overall $[Ca^{2+}]_i$ and contractile response are expected to be small. That is also evident from a large half-saturation constant ($K_{cGMP,NCX}$) in the cGMP-dependent function $R_{NCX,cGMP}$. However, the overall effect should be tested by integrating all mechanisms in a whole-cell-like VSMC model.

4.4 The model of cGMP-mediated current through the Na^+/K^+-ATPase (NKA)

The NKA pumps Na^+ out and K^+ in and has stoichiometry 3 Na^+:2 K^+. Jacobsen et al. [50] modeled the whole-cell electric current through NKA (I_{NaK}) as in [68]:

$$I_{NaK} = I_{NaK,max} \frac{[K^+]_i}{[K^+]_i + K_{K,NaK}} \frac{[Na^+]_i^{n_{NaK,Na}}}{[Na^+]_i^{n_{NaK,Na}} + K_{Na,NaK}^{n_{NaK,Na}}} \frac{V_m + \Delta V_1}{V_m + \Delta V_2}, \tag{17}$$

whereby the maximal current ($I_{NaK,max}$) is considered as linearly cGMP-dependent:

$$I_{NaK,max} = k_{1,NaK,cGMP}[cGMP] - k_{2,NaK,cGMP}. \tag{18}$$

All parameter descriptions and their values are presented in **Table 4**.

In terms of membrane potential, increased NKA activity hyperpolarizes the membrane and enhances the Ca^{2+} influx through VOCC, which is similar to the effect of cGMP on BKCa. The effect of cGMP/PKG on NKA has not been studied often. The mathematical model is built on a single measurement on purified pig renal NKA at one single concentration of cGMP, which in addition to PKG increased the activity 1.6-fold. cGMP alone did not change the activity, and PKG alone increased it 1.2-fold [76]. Due to the lack of credible measurements, the reliability of this model is limited.

Parameter	Description	Values [51]
$I_{NCX,s}$	Current scaling factor	0.0487–0.487 pA
d_{NCX}	Denominator constant	3×10^{-4}
γ	Voltage-dependence parameter	0.45
$f_{NCX,cGMP}$	Additional fold increase in electric current due to cGMP	0.55
$K_{cGMP,NCX}$	Half saturation constant in cGMP-dependent term	45 μM

Table 3.
Parameter values for the cGMP-dependent Na^+/ Ca^{2+} exchange (NCX) current.

Parameter	Description	Values [50]
$K_{K,NaK}$	Half-saturation constant	1 mM
$K_{Na,NaK}$	Half-saturation constant	11 mM
$n_{NaK,Na}$	Hill coefficient	1.5
ΔV_1	Electric potential shift	150 mV
ΔV_2	Electric potential shift	200 mV
$k_{1,NaK,cGMP}$	cGMP-concentration weighted electric current	30 pA/μM
$k_{2,NaK,cGMP}$	Electric current constant	30 pA

Table 4.
Parameter values for the cGMP-dependent current trough Na^+/K^+-ATPase (NKA).

4.5 The model of cGMP-mediated current through the $Na^+/K^+/Cl^-$ cotransporter (NKCC)

Instead of cGMP-dependent NKA, Kapela et al. [51] modeled the cGMP influence on the $Na^+/K^+/Cl^-$ cotransport (NKCC) having the 1:1:2 stoichiometry. The expression describing the electric current for a particular ion (I^i_{NaKCl}, where i is either Na, K, or Cl) was taken from [77] and upgraded with a cGMP dependency. According to [77], electric currents of individual ions are defined according to the valence (Z) and the stoichiometry:

$$I^{Na}_{NaKCl} = I^{K}_{NaKCl} = -\frac{1}{2} I^{Cl}_{NaKCl}. \tag{19}$$

Here only the electric current for Cl^- (I^{Cl}_{NaKCl}) is written:

$$I^{Cl}_{NaKCl} = -I_{NaKCl} Z_{Cl} R_{NaKCl,cGMP} \ln\left(\frac{[Na^+]_o}{[Na^+]_i}\frac{[K^+]_o}{[K^+]_i}\left(\frac{[Cl^-]_o}{[Cl^-]_i}\right)^2\right), \tag{20}$$

where Z_{Cl} is the valence of Cl^-, I_{NaKCl} is a cotransport current coefficient, and $[Na^+]$, $[K^+]$ and $[Cl^-]$ are the corresponding concentrations outside and inside (subscripts o and i, respectively) of the cell. $R_{NaKCl,cGMP}$ represents the cGMP-dependent regulation factor that is defined as:

$$R_{NaKCl,cGMP} = 1 + f_{NaKCl,cGMP} \frac{[cGMP]}{[cGMP] + K_{cGMP,NaKCl}}, \tag{21}$$

where $f_{NaKCl,cGMP}$ is a fold-increase in cotransport current due to cGMP. All parameters and their values are presented in **Table 5**.

Very little is known about the effect of cGMP on the NKCC. The model is more or less built on one single reference [49], which also offers limited information for

Parameter	Description	Values [51]
I_{NaKCl}	Cotransport current coefficient	0.106 pA
$f_{NaKCl,cGMP}$	Additional fold-increase in electric current due to cGMP	3.5
$K_{cGMP,NaKCl}$	Half-saturation constant in cGMP-dependent factor	6.4 μM

Table 5.
Parameter values for the cGMP-dependent $Na^+/K^+/Cl^-$ cotransport (NKCC) current.

determining the reliable parameter values. The knowledge of the overall impact of NKCC on VSMC contraction is lacking. Hence, their inclusion in the cGMP-dependent mechanisms seems speculative.

4.6 The model of cGMP-mediated Ca^{2+} flux through the sarco−/endo-plasmic reticulum Ca^{2+}-ATPase (SERCA)

Here we present a novel model of cGMP-dependent activation of the SERCA pump based on the solid-state NMR spectroscopy measurements [35] and the measurements performed on the isolated gastric SMC [36]. The former experiment [35] revealed the physical interactions between the SERCA and the PLB in either a phosphorylated or dephosphorylated state, and the latter experiment [36] offered the results on the increase in Ca2+ uptake as a function of cGMP. The experiments performed on isolated lipid bilayer-bound proteins revealed that the PLB-dependent SERCA activity regulation is allosteric and that SERCA activity depends on the transient conformational equilibrium states of PLB [35]. It was found that phosphorylation at Ser16 of PLB shifts the conformation of PLB towards a more extended and SERCA-bound state, which is non-inhibitory [35]. Phosphorylation of PLB was induced by β-adrenergic stimulation, and it was supposed that the phosphorylation was cAMP/PKA dependent [35]. However, the cGMP/PKG-I dependent phosphorylation of PLB at Ser16 in contact with SERCA was previously shown *in vitro* [33]. Gustavsson et al. [35] proposed that PLB does not function as a simple on/off switch of SERCA. Still, its different conformational equilibrium states exert a gradual control on SERCA activity. PLB phosphorylation does not cause complete dissociation of PLB from SERCA, but it influences the conformational equilibrium of PLB's regulatory domain and shifts its populations towards the non-inhibitory state. That relieves the inhibition of SERCA [35]. According to [35], different PLB/SERCA states exhibit functioning that follows Michaelis–Menten kinetics with the same Hill coefficient (n) and same (V_{max}) but different half-saturation constant (K_m), which is lower for higher relaxation-agonist level. Since the effect of cGMP solely on the half-saturation constant could not explain the increase in Ca^{2+} uptake as a function of high cGMP concentration that was observed *in vitro* in gastric SMC [36], we upgraded the model also by adding a cGMP-dependent regulatory factor into the parameter V_{max} of the standard Michaelis–Menten kinetics, which for SERCA reads:

$$J_{SERCA} = V_{SERCA,min} R_{SERCA,cGMP} \frac{\left[Ca^{2+}\right]_i^{n_{SERCA,Ca}}}{\left[Ca^{2+}\right]_i^{n_{SERCA,Ca}} + R_{Ca,cGMP}^{n_{SERCA,Ca}} K_{Ca,SERCA,max}^{n_{SERCA,Ca}}}, \quad (22)$$

where $R_{SERCA,cGMP}$ is a cGMP-dependent pumping rate regulatory factor, which is according to [36] an increasing Hill function superimposed on the basal pumping rate $V_{SERCA,min}$. The Hill function represents the best fit to the measured data of cGMP dependent increase in Ca^{2+} uptake [36]:

$$R_{SERCA,cGMP} = 1 + f_{SERCA,cGMP} \frac{[cGMP]^{n_{SERCA,cGMP,V}}}{[cGMP]^{n_{SERCA,cGMP,V}} + K_{cGMP,SERCA,V}^{n_{SERCA,cGMP,V}}}. \quad (23)$$

$R_{Ca,cGMP}$ is a cGMP-dependent half-saturation constant regulatory factor in the Eq. (22), which is according to the measurements [35] a decaying Hill function:

$$R_{Ca,cGMP} = 1 - f_{Ca,cGMP} \frac{[cGMP]^{n_{SERCA,cGMP,K}}}{[cGMP]^{n_{SERCA,cGMP,K}} + K_{cGMP,SERCA,K}^{n_{SERCA,cGMP,K}}}. \quad (24)$$

Parameter	Description	Value	References
$n_{SERCA,Ca}$	Hill coefficient	2.5	[50]
$V_{SERCA,min}$	Minimal Ca^{2+} pumping rate	1.88×10^3 μM/s	[50]
$f_{SERCA,cGMP}$	Additional fold increase in SERCA activity due to cGMP	1.44	Recalculated by fitting from [36]
$K_{cGMP,SERCA,V}$	Half-saturation constant in the cGMP-dependent regulatory Hill function	1.44×10^2 μM	Recalculated by fitting from [36]
$n_{SERCA,cGMP,V}$	Hill coefficient	0.092	Recalculated by fitting from [36]
$K_{Ca,SERCA,max}$	Maximal value of SERCA half-saturation constant	0.07 μM	[50]
$f_{Ca,cGMP}$	Additional fold decrease in SERCA activity due to cGMP	70	Recalculated by fitting from [36]
$K_{cGMP,SERCA,K}$	Half saturation constant in the cGMP-dependent regulatory Hill function	0.1 μM	Recalculated by fitting from [35]
$n_{SERCA,cGMP,K}$	Hill coefficient	1.2	Recalculated by fitting from [35]

Table 6.
Parameter values for the cGMP-dependent Ca^{2+} efflux via SERCA.

All parameter values and their descriptions are presented in **Table 6**.

It has to be noted that the parameter values for Eq. (25) were determined by the best fit to only three measured values from [35], and that $K_{SERCA,Ca,max}$ is considered the same as in the existing model for VSMC [50]. In the case of $V_{SERCA,min}$, the best fit was done to five measured points [36].

The significance of the cGMP effect on SERCA is still debated, and it is challenging to consider it independently of other $[Ca^{2+}]_i$-off mechanisms. It is suggested [78] that cGMP-dependent SERCA activity can play a significant role in modulating smooth muscle $[Ca^{2+}]_i$, but its role in the cGMP-mediated relaxation is minor. Therefore, it would be worth testing the significance of that mechanism on the whole-cell-like VSMC model.

4.7 The model of cGMP-mediated current through the plasma membrane Ca^{2+}-ATPase (PMCA)

Yoshida et al. [40] demonstrated that PKG phosphorylated and stimulated PMCA in a concentration-dependent manner. The experiment was conducted on isolated and purified PMCA from the porcine aorta. Much smaller - physiological cGMP concentration, 1 μM, than in previous experiments (500 μM) [38, 39], was added to 10 μg/mL (roughly 0.2 μM) PKG at different free Ca^{2+} concentrations. That increased PMCA activity by approximately 3-fold over the whole range of Ca^{2+} concentrations and slightly shifted the pumping activity towards the left. cGMP alone did not affect the pump activity [40]. In modeling these effects, we use a similar approach as for SERCA, which obeys Michaelis–Menten kinetics. However, previous studies [50, 79] also included weak membrane-potential-dependence, which we also consider here:

$$I_{PMCA} = I_{PMCA,min} R_{PMCA,cGMP} \frac{\left[Ca^{2+}\right]_i^{n_{PMCA,Ca}}}{\left[Ca^{2+}\right]_i^{n_{PMCA,Ca}} + K_{Ca,PMCA}^{n_{PMCA,Ca}}} \left(1 + \frac{V_m - k_\beta}{k_\alpha}\right), \quad (25)$$

Parameter	Description	Value	References
$n_{PMCA,Ca}$	Hill coefficient	0.6	Recalculated by fitting from [40]
$I_{PMCA,min}$	Minimal Ca^{2+} pumping current	0.90 pA	[50]
$K_{Ca,PMCA}$	Half-saturation constant in Ca^{2+}-dependent factor	0.18 μM	Recalculated by fitting from [40]
k_β	PMCA voltage sensitivity constant	−100 mV	[50]
k_α	PMCA voltage sensitivity constant	250 mV	[50]
$f_{PMCA,cGMP}$	Additional fold-increase in electric current due to cGMP	3	Recalculated by fitting from [40]
$K_{cGMP,PMCA}$	Half-saturation constant in the cGMP-dependent regulatory Hill function	0.50 μM	Recalculated by fitting from [40]
$n_{PMCA,cGMP}$	Hill coefficient	1.7	Recalculated by fitting from [40]

Table 7.
Parameter values for the cGMP-dependent Ca^{2+} current via PMCA.

where $I_{PMCA,min}$ is a minimal pumping rate translated into electric current, which is, according to [40], a function of PKG. Yoshida et al. [40] conducted all their experiments at variable PKG concentrations and 5 to 20 times higher cGMP concentration. Since all our functions were written as cGMP-dependent, we translate PKG concentrations into cGMP by considering the active PKG:cGMP molar ratio 1:4. The Hill function fitted to measured data [40] is superimposed on the basal pumping current $I_{PMCA,min}$ and is here represented as a cGMP-dependent regulatory factor:

$$R_{PMCA,cGMP} = 1 + f_{PMCA,cGMP} \frac{[cGMP]^{n_{PMCA,cGMP}}}{[cGMP]^{n_{PMCA,cGMP}} + K_{cGMP,PMCA}^{n_{PMCA,cGMP}}}. \quad (26)$$

Parameter values and their descriptions are presented in **Table 7**.

In Eq. (25), $K_{Ca,PMCA}$ is a half-saturation constant. The value was determined by fitting the Hill function to two sets of measured data [40], the control case, and the PKG-dependent case, with 0.2 μM PKG and 1 μM cGMP. For the former case, the value is 0.22 μM, and for the latter case, it is 0.14 μM. Since the change is rather small and there are only two measured values available, we do not assume cGMP dependency in this case. That decision is also supported by the results of [39] where the left-shift in that value was only by 27% at supramaximal membrane-permeable cGMP analog concentration (500 μM). We propose here the average value. Elsewhere the value is similar (0.2 μM) [50, 79] and 0.17 μM [51]. $n_{PMCA,Ca}$ is also determined by fitting to the same set of measured data [40]. The values were 0.7 and 0.5 for the control and the PKG-dependent case, respectively. We propose here an average. Value 1 was used elsewhere [50, 51, 79]. Fold-increase in electric current due to cGMP is quite large and might impact the $[Ca^{2+}]_i$, which the whole-cell-like model could demonstrate.

4.8 The model of cGMP-mediated Ca^{2+} flux through the inositol 1,4,5-trisphosphate (IP_3) receptor channels type 1 (IP_3R1)

4.8.1 Variant A

The proposed model for cGMP-mediated IP_3R1 deactivation is also presented here for the first time. The framework of the proposed mechanism is the model of

the Ca^{2+} efflux via IP_3R1 as proposed by [50]. That model is upgraded here according to the experimental data of [36], with an additional regulatory factor $R_{IR1,cGMP}$, which accounts for the drop in Ca^{2+} release after IP_3 stimulation with increasing cGMP levels [36]. General description of the Ca^{2+} flux across the SR membrane through the IP_3R1 channels (J_{IR1}) follows [50]:

$$J_{IR1} = g_{IR1} P_{IR1} \left(\left[Ca^{2+}\right]_{SR} - \left[Ca^{2+}\right]_i \right), \tag{27}$$

where g_{IR1} is an overall maximal rate of the channel permeability and P_{IR1} is the channel open probability, which is a biphasic bell-shaped function of $[Ca^{2+}]_i$, and is also dependent on the cytosolic IP_3 and sarcoplasmic Ca^{2+} concentrations ($[IP_3]$ and $[Ca^{2+}]_{SR}$, respectively). It is modeled as in [50, 80]:

$$P_{IR1} = f_{IR1,A} \left(1 - f_{IR1,I}\right) R_{IR1,cGMP} \frac{[IP_3]^{n_{IP3}}}{[IP_3]^{n_{IP3}} + K_{IP3}^{n_{IP3}}} \frac{\left[Ca^{2+}\right]_{SR}^{n_{SR}}}{\left[Ca^{2+}\right]_{SR}^{n_{SR}} + K_{Ca,SR}^{n_{SR}}}. \tag{28}$$

The regulatory factor $R_{IR1,cGMP}$ is a decaying Hill function that depends on the cGMP concentration and is an upgrade from the previous model [50]. The proposed function is the best fit to the measured decay of IP_3-induced Ca^{2+} release as a function of cGMP concentration in isolated gastric SMC [36]:

$$R_{IR1,cGMP} = 1 - f_{IR1,cGMP} \frac{[cGMP]^{n_{IR1,cGMP}}}{[cGMP]^{n_{IR1,cGMP}} + K_{cGMP,IR1}^{n_{IR1,cGMP}}}, \tag{29}$$

where $f_{IR1,cGMP}$ is an additional fold decrease in the channel open probability due to cGMP. $f_{IR1,A}$, and $f_{IR1,I}$ in Eq. (29) are the fractions of the channel population occupied by $[Ca^{2+}]_i$ at the activation sites and inactivation sites, respectively. In this way, the bell-shaped dependency on $[Ca^{2+}]_i$ is achieved. Since activation is a fast process, it is considered to be in the equilibrium:

$$f_{IR1,A} = \frac{\left[Ca^{2+}\right]_i^{n_A}}{\left[Ca^{2+}\right]_i^{n_A} + K_{Ca,A}^{n_A}}, \tag{30}$$

whereas the Ca^{2+}-dependent IP_3R1 inhibition is considered as slow and is therefore modeled with the first-order kinetics as in Eq. (3):

$$\frac{df_{IR1,I}}{dt} = \frac{\bar{f}_{IR1,I} - f_{IR1,I}}{\tau_{IR1,I}}, \tag{31}$$

where $\bar{f}_{IP31,I}$ is the fraction of the inhibited state in equilibrium, which follows a Hill function:

$$\bar{f}_{IR1,I} = \frac{\left[Ca^{2+}\right]_i^{n_I}}{\left[Ca^{2+}\right]_i^{n_I} + K_{Ca,I}^{n_I}}. \tag{32}$$

Description of all parameters and their values are presented in **Table 8**.

4.8.2 Variant B

Other results of Murthy and Zhou [20] provide another possible model description of cGMP-dependent IP_3R1 inhibition. The experiment offers direct PKG or

Parameter	Description	Value	References
g_{IR1}	Maximal permeability rate of the channel	30 s^{-1}	[50]
K_{IP3}	Half saturation constant in the IP_3-dependent regulatory Hill function	0.65 μM	[50]
$K_{Ca,SR}$	Half saturation constant in the sarcoplasmic Ca^{2+}-dependent regulatory Hill function	2×10^3 μM	[50]
n_{IP3}	Hill coefficient	4	[50]
n_{SR}	Hill coefficient	2	[50]
$f_{IR1,cGMP}$	Additional fold decrease in the channel open probability due to cGMP	0.645	Recalculated by fitting from [36]
$K_{cGMP,IR1}$	Half saturation constant in the cGMP-dependent regulatory Hill function	24.6 μM	Recalculated by fitting from [36]
$n_{IR1,cGMP}$	Hill coefficient	0.47	Recalculated by fitting from [36]
$K_{Ca,A}$	Half saturation constant in the cytosolic Ca^{2+}-dependent regulatory Hill function	0.13 μM	[50]
n_A	Hill coefficient	4	[50]
$\tau_{IR1,I}$	Characteristic transition time	6.0 s	[50]
$K_{Ca,I}$	Half saturation constant in the cytosolic Ca^{2+}-dependent regulatory Hill function	0.35 μM	[50]
n_I	Hill coefficient	4	[50]

Table 8.
Parameter values for the cGMP and IP_3 -dependent open probability of IP_3R1 – Variant a.

cGMP dependency of IP_3-dependent Ca^{2+} flux. The cGMP/PKG mediated phosphorylation of IP_3R1 in microsomes was confirmed in the accompanying experiment by immunoprecipitation. Hence, Murthy and Zhou [20] measured Ca^{2+} release through the phosphorylated IP_3R1 within smooth muscle microsomes at different IP_3 concentrations. Prior to measurements, microsomes were either treated with 0.5 μM PKG-Iα holoenzyme and 10 μM cGMP or left intact (control). Ca^{2+} release was determined from the decrease in the steady-state microsomal radioactive Ca^{2+} isotope content. In this way, two dose–response curves were obtained [20]. Their best fits with a Hill function reveal almost the same Hill coefficients (0.49 and 0.42, for the control and cGMP/PKG treated case, respectively) and the same V_{max} (100%) but significantly different half-saturation constants Km, 1.17×10^{-3} μM and 2.35 μM, for the control and the cGMP/PKG treated case, respectively. These two measured values represent two points to which any function could virtually be fitted. Since this is highly unrealistic, we propose the use of competitive, reversible enzyme inhibition kinetics, where cGMP represents an inhibitor in the IP_3-dependent open probability function:

$$OP_{IP3,cGMP} = \frac{[IP_3]^{n_{IP3}}}{[IP_3]^{n_{IP3}} + K_{IP3,cGMP}^{n_{IP3}}}, \tag{33}$$

where $K_{IP3,cGMP}$ is:

$$K_{IP3,cGMP} = K_{IP3,0}\left(1 + \frac{[cGMP]}{K_{i,cGMP}}\right). \tag{34}$$

Parameter	Description	Value	References
$K_{IP3,0}$	Half-saturation constant in the IP_3-dependent regulatory Hill function	0.65 μM	[50]
n_{IP3}	Hill coefficient	4	[50]
$K_{i,cGMP}$	Apparent inhibition constant for cGMP-dependent inhibition of IP_3-dependent open probability of IP_3R1	5.0×10^{-3} μM	Recalculated from [20]
$K_{i,PKG}$	Apparent inhibition constant for PKG-dependent inhibition of IP_3-dependent open probability of IP_3R1	0.25×10^{-3} μM	Recalculated from [20]

Table 9.
Parameter values for the cGMP and IP_3 -dependent open probability of IP_3R1 – Variant B.

The parameter$K_{i,cGMP}$ is recalculated from [20] according to:

$$K_{i,cGMP} = \frac{K_{IP3,c}[cGMP]_0}{K_{IP3,cGMP,i} - K_{IP3,c}}, \tag{35}$$

where $K_{IP3,cGMP,i}$ = 2.35 μM, which is a measured half-saturation constant treated with $[cGMP]_0$ = 10 μM, and $K_{IP3,c}$ = 1.17×10^{-3} μM, which is the corresponding value at control experiment without added cGMP. Eq. (37) gives $K_{i,cGMP}$ = 5.0×10^{-3} μM. The same calculation in which PKG is replacing cGMP in Eqs. (32)–(34) with the value $[PKG]_0$ =0.50 μM yields $K_{i,PKG}$ = 0.25×10^{-3} μM. The summary of parameter values accounting for $OP_{IP3,cGMP/PKG}$ as a function of either cGMP or PKG is presented in **Table 9**.

We offer here two different variants of the mathematical descriptions for the cGMP impact on the IP_3R1. Variant A seems more realistic as it contains the description with saturating Hill function. On the other hand, variant B takes into account the linear relationship on cGMP concentration, which might be questionable at high cGMP concentrations. However, variant B offers an insight into the strength of the inhibition on IP_3R1 exerted by cGMP. $K_{i,cGMP}$ and $K_{i,PKG}$ values indicate very strong inhibition. It is also worth mentioning that such an effect might also arise from the experimental conditions since they were performed on the isolated microsomes [20]. Before actual inclusion of either of both mechanisms into a whole-cell-like model of VSMC, their careful model evaluation at different dynamical levels of $[Ca^{2+}]_i$ signaling, such as membrane potential, basal $[Ca^{2+}]_i$, different shapes and frequencies of $[Ca^{2+}]_i$ signal, would be required.

4.9 The model of cGMP-mediated Ca^{2+}-desensitization of the contractile apparatus

Modeling of cGMP/PKG- dependent Ca^{2+}-desensitization was first introduced by Yang et al. [67], who considered that MLCP is directly activated by cGMP. They modified the 4-state latch bridge model introduced by Hai and Murphy [13] by considering a simple theoretical description of Ca^{2+}/CaM-dependent MLCK activation and MLCP dependent dephosphorylation [67]. They also reduced the model from 4 to 2 states of myosin species, phosphorylated and dephosphorylated (M_p and M, respectively), being in equilibrium. Hence, the relative level of phosphorylated myosin (M_p) was expressed as:

$$M_p = \frac{k_{cat,MLCK}}{k_{cat,MLCK} + R_{MLCP,cGMP}k_{cat,MLCP,b}}, \tag{36}$$

where $k_{cat,MLCK}$ is $[Ca^{2+}]_i$ dependent rate of phosphorylation (see [67]) and, $k_{cat,MLCP,b}$ is a basal dephosphorylation rate that is multiplied by the cGMP-dependent regulatory factor:

$$R_{MLCP,cGMP} = 1 + f_{MLCP,cGMP} \frac{[cGMP]^{n_{MLCP}}}{[cGMP]^{n_{MLCP}} + K_{cGMP,MLCP}^{n_{MLCP}}}, \tag{37}$$

where $f_{cat,MLCP}$ is an additional fold-increase in the MLCP-mediated M_p dephosphorylation rate due to cGMP. $K_{cGMP,MLCP}$ is a half-saturation constant within cGMP-dependent regulatory Hill function with a Hill coefficient n_{MLCP}.

The model of Yang et al. [67] demonstrated cGMP-mediated Ca^{2+}-desensitization by shifting the equilibrium MLC phosphorylation and force curves vs. $[Ca^{2+}]_i$ to the right. However, the model was not used to simulate the time-dependent phosphorylation and force development. In this context, the model would not accurately predict the results since Ca^{2+}-dependent MLCK activation could not be considered as a fast process [81, 82]. Also, the simplification from 4 to 2 states is neither reasonable nor relevant if the model would account for the time-dependent variables. Hence, we propose another modeling approach to tackle the cGMP-dependent activation of MLCP. The proposed model considers the Michaelis–Menten-type of enzyme kinetics for the rate of MLC dephosphorylation within the 4-state latch bridge kinetic scheme [83], yielding the velocity of MLCP dependent dephosphorylation (V_{MLCP}) of both phosphorylated myosin species, attached and detached to actin, $AM_{p,}$ and M_p, respectively:

$$V_{MLCP} = \frac{d[M_p]}{dt} + \frac{d[AM_p]}{dt} = \frac{R_{MLCP,cGMP} k_{cat,MLCP,b} [MLCP]_{tot}}{[M_p] + [AM_p] + K_{MLCP}} ([M_p] + [AM_p]), \tag{38}$$

where $[MLCP]_{tot}$ is the total MLCP concentration, K_{MLCP} is a Michaelis–Menten constant, and $k_{cat,MLCP}$ is a catalytic rate constant, for which we consider to be cGMP-dependent as proposed by [67] in Eq. (35). All current parameters are presented in **Table 10**.

A similar modeling approach for ROCK-dependent sensitization of the contractile apparatus was used in our previous work [64]. The whole model for all Ca^{2+}/CaM/MLCK interactions, all myosin species, and the time-dependent force development is presented in different variants elsewhere [64, 81, 82, 84] and it comprises more than 12 differential equations. That is a minor drawback of the model, but the model proved itself in describing time-dependent force generation in rat airway smooth muscle cells [64, 82]. Such an extended model would also allow the

Parameter	Description	Value	References
$k_{MLCP,b}$	Basal dephosphorylation rate	8 s^{-1}	[64]
$f_{MLCP,cGMP}$	Additional fold increase in dephosphorylation rate due to cGMP	1	[64]
n_{MLCP}	Hill ceofficient	2	[67]
$K_{cGMP,MLCP}$	Half saturation constant in a cGMP-dependent regulatory Hill function	5.5 μM	[67]
K_{MLCP}	Michaelis–Menten constant	10 μM	[81]
$[MLCP]_{tot}$	Total MLCP concentration	2 μM	[81]

Table 10.
Parameter values for cGMP-dependent Ca^{2+}-desensitization of the contractile apparatus.

modeling of other cGMP/PKG-mediated mechanisms of MLCP and MLCK regulation by considering several different microscopic states of these two enzymes, such as different phosphorylated states, interaction with telokin, CPI-17, etc. That would allow the interconnection of different signal pathways and, hence, the simulation of the effects of various agonists and inhibitors.

5. Conclusion

This work discusses previous and provides the novel cGMP/PKG-dependent mechanisms at the molecular level accounting for their potential use in comprehensive whole-cell-like models of vascular smooth muscle contraction. Much has been done in the fields of measurements and modeling of the cGMP/PKG effects on the individual $[Ca^{2+}]_i$ encoding and decoding mechanisms implicated in VSMC contractility. However, especially in the modeling part, there is still room for improvement and upgrading the existing models and building even multi-cellular [85, 86] and systems-pharmacology based models [87]. We should also take into consideration the importance of coupling the models of vascular smooth muscle cells to endothelial cells that, in response to the shear stress of blood flow, produce NO and other contractile and relaxation mediators [88, 89]. Moreover, the models would enable simulations at the tissue and organ level [90]. However, many of such multi-scale models are weak in describing mechanisms at the molecular level. That is not an easy task since the number of variables and parameters and the model complexity can increase tremendously. The other possibility to tackle that web of interrelated interactions is by complex network approach [91]. However, a dynamic modeling approach, as presented here, which is currently presented only at the level of individual fluxes that need to be assembled into a comprehensive model, offers many more options for studying the temporal dynamical behavior of the system functioning, either under physiological or pathological conditions or after pharmacological intervention. The remarkable advantage and added value of such mathematical models is that they describe the processes as dynamic ones. They often do not consider only one single process but take into account mutual interactions between several highly interrelated variables. In this way, they reach beyond the intuitive thinking of direct and inverse proportions between certain variables, which is often the case when interpreting the experimental results. However, models hide other pitfalls, such as excessive simplicity or complexity, unfounded predictions, prejudging, unawareness of the model's limitations, and transfer of models between different cell types and organisms, and much more. Nevertheless, they represent a useful tool for in-depth insight into the system's dynamical functioning, distinguishing essential from nonessential mechanisms, and last but not least, for highlighting the targets of pharmacological intervention.

Acknowledgements

The author acknowledges the support of the Slovenian Research Agency (ARRS) grant P1–0055.

Conflict of interest

The author declares no conflict of interest.

DOI: http://dx.doi.org/10.5772/intechopen.97708

Author details

Aleš Fajmut
Faculty of Natural Sciences and Mathematics and Faculty of Health Sciences, University of Maribor, Maribor, Slovenia

*Address all correspondence to: ales.fajmut@um.si

References

[1] Kots AY, Martin E, Sharina IG, Murad F. A short history of cGMP, guanylyl cyclases, and cGMP-dependent protein kinases. In: Schmidt HH, Hofmann F, Stasch J-P, editors. cGMP: Generators, Effectors and Therapeutic Implications. Handbook of Experimental Pharmacology. 191. Heidelberg: Springer; 2009. p. 1-14. DOI:10.1007/978-3-540-68964-5_1.

[2] Golshiri K, Ataei Ataabadi E, Portilla Fernandez EC, Jan Danser A, Roks AJ. The importance of the nitric oxide-cGMP pathway in age-related cardiovascular disease: Focus on phosphodiesterase-1 and soluble guanylate cyclase. Basic & clinical pharmacology & toxicology. 2020;127 (2):67-80. DOI:10.1111/bcpt.13319.

[3] Hofmann F, Feil R, Kleppisch T, Schlossmann J. Function of cGMP-dependent protein kinases as revealed by gene deletion. Physiological reviews. 2006;86(1):1-23. DOI:10.1152/ physrev.00015.2005.

[4] Tsai EJ, Kass DA. Cyclic GMP signaling in cardiovascular pathophysiology and therapeutics. Pharmacology & therapeutics. 2009;122 (3):216-238. DOI:10.1016/j. pharmthera.2009.02.009.

[5] Murad F. Cellular signaling with nitric oxide and cyclic GMP. Brazilian journal of medical and biological research. 1999;32(11):1317-1327. DOI: 10.1590/s0100-879x1999001100001.

[6] Ando J, Yamamoto K. Flow detection and calcium signalling in vascular endothelial cells. Cardiovascular research. 2013;99(2):260-268. DOI: 10.1093/cvr/cvt084.

[7] Putney JW, Broad LM, Braun F-J, Lievremont J-P, Bird GSJ. Mechanisms of capacitative calcium entry. Journal of cell science. 2001;114(12):2223-2229.

[8] Martinac B. Mechanosensitive ion channels: molecules of mechanotransduction. Journal of Cell Science. 2004;117(12):2449-2460. DOI: 10.1242/jcs.01232.

[9] Ando J, Yamamoto K. Vascular mechanobiology endothelial cell responses to fluid shear stress. Circulation Journal. 2009;73(11): 1983-1992. DOI:10.1253/circj.cj-09-0583.

[10] Francis SH, Blount MA, Corbin JD. Mammalian cyclic nucleotide phosphodiesterases: molecular mechanisms and physiological functions. Physiological reviews. 2011; 91(2):651-690. DOI:10.1152/ physrev.00030.2010.

[11] Hill MA, Meininger GA, Davis MJ, Laher I. Therapeutic potential of pharmacologically targeting arteriolar myogenic tone. Trends in pharmacological sciences. 2009;30(7): 363-374. DOI:10.1016/j. tips.2009.04.008.

[12] Somlyo AP, Somlyo AV. Ca2+ sensitivity of smooth muscle and nonmuscle myosin II: modulated by G proteins, kinases, and myosin phosphatase. Physiological reviews. 2003.

[13] Hai C-M, Murphy RA. Cross-bridge phosphorylation and regulation of latch state in smooth muscle. American Journal of Physiology-Cell Physiology. 1988;254(1):C99-C106. DOI:10.1152/ ajpcell.1988.254.1.c99.

[14] Brozovich F, Nicholson C, Degen C, Gao YZ, Aggarwal M, Morgan KG. Mechanisms of vascular smooth muscle contraction and the basis for pharmacologic treatment of smooth muscle disorders. Pharmacological reviews. 2016;68(2):476-532. DOI: 10.1124/pr.115.010652.

[15] Marhl M, Noble D, Roux E. Modeling of molecular and cellular mechanisms involved in Ca2+ signal encoding in airway myocytes. Cell Biochemistry and Biophysics. 2006 2006/11/01;46(3):285-302. DOI: 10.1385/cbb:46:3:285.

[16] Gao Y. Biology of vascular smooth muscle: vasoconstriction and dilatation: Springer; 2017. DOI:10.1007/978-981-10-4810-4.

[17] Kim JJ, Lorenz R, Arold ST, Reger AS, Sankaran B, Casteel DE, et al. Crystal structure of PKG I: cGMP complex reveals a cGMP-mediated dimeric interface that facilitates cGMP-induced activation. Structure. 2016;24 (5):710-720. DOI:10.1016/j.str.2016.03.009.

[18] Bonnevier J, Fässler R, Somlyo AP, Somlyo AV, Arner A. Modulation of Ca2 + sensitivity by cyclic nucleotides in smooth muscle from protein kinase G-deficient mice. Journal of Biological Chemistry. 2004;279(7):5146-5151. DOI: 10.1074/jbc.m306532200.

[19] Schlossmann J, Ammendola A, Ashman K, Zong X, Huber A, Neubauer G, et al. Regulation of intracellular calcium by a signalling complex of IRAG, IP 3 receptor and cGMP kinase Iβ. Nature. 2000;404 (6774):197-201. DOI:10.1038/35004606.

[20] Murthy KS, Zhou H. Selective phosphorylation of the IP3R-I in vivo by cGMP-dependent protein kinase in smooth muscle. American Journal of Physiology-Gastrointestinal and Liver Physiology. 2003;284(2):G221-G230. DOI:10.1152/ajpgi.00401.2002.

[21] Geiselhöringer A, Werner M, Sigl K, Smital P, Wörner R, Acheo L, et al. IRAG is essential for relaxation of receptor-triggered smooth muscle contraction by cGMP kinase. The EMBO journal. 2004;23(21):4222-4231. DOI: 10.1038/sj.emboj.7600440.

[22] Ammendola A, Geiselhöringer A, Hofmann F, Schlossmann J. Molecular determinants of the interaction between the inositol 1, 4, 5-trisphosphate receptor-associated cGMP kinase substrate (IRAG) and cGMP kinase Iβ. Journal of Biological Chemistry. 2001; 276(26):24153-24159. DOI:10.1074/jbc.m101530200.

[23] Masuda W, Betzenhauser MJ, Yule DI. InsP3R-associated cGMP kinase substrate determines inositol 1, 4, 5-trisphosphate receptor susceptibility to phosphoregulation by cyclic nucleotide-dependent kinases. Journal of Biological Chemistry. 2010;285(48):37927-37938. DOI:10.1074/jbc.m110.168989.

[24] Desch M, Sigl K, Hieke B, Salb K, Kees F, Bernhard D, et al. IRAG determines nitric oxide-and atrial natriuretic peptide-mediated smooth muscle relaxation. Cardiovascular research. 2010;86(3):496-505. DOI: 10.1093/cvr/cvq008.

[25] Tang M, Wang G, Lu P, Karas RH, Aronovitz M, Heximer SP, et al. Regulator of G-protein signaling-2 mediates vascular smooth muscle relaxation and blood pressure. Nature medicine. 2003;9(12):1506-1512. DOI: 10.1038/nm958.

[26] Xia C, Bao Z, Yue C, Sanborn BM, Liu M. Phosphorylation and regulation of G-protein-activated phospholipase C-β3 by cGMP-dependent protein kinases. Journal of Biological Chemistry. 2001; 276(23):19770-19777. DOI:10.1074/jbc.m006266200.

[27] Sun X, Kaltenbronn KM, Steinberg TH, Blumer KJ. RGS2 is a mediator of nitric oxide action on blood pressure and vasoconstrictor signaling. Molecular pharmacology. 2005;67(3): 631-639. DOI:10.1124/mol.104.007724.

[28] Ruiz-Velasco V, Zhong J, Hume JR, Keef KD. Modulation of Ca2+ channels by cyclic nucleotide cross activation of

opposing protein kinases in rabbit portal vein. Circulation Research. 1998;82(5): 557-565. DOI:10.1161/01.res.82.5.557.

[29] Harraz OF, Welsh DG. Protein kinase A regulation of T-type Ca2+ channels in rat cerebral arterial smooth muscle. Journal of cell science. 2013;126 (13):2944-2954. DOI:10.1242/jcs.128363.

[30] Harraz OF, Brett SE, Welsh DG. Nitric oxide suppresses vascular voltage-gated T-type Ca2+ channels through cGMP/PKG signaling. American Journal of Physiology-Heart and Circulatory Physiology. 2014;306 (2):H279-H285. DOI:10.1152/ ajpheart.00743.2013.

[31] Chen J, Crossland RF, Noorani MM, Marrelli SP. Inhibition of TRPC1/TRPC3 by PKG contributes to NO-mediated vasorelaxation. American journal of physiology-Heart and circulatory physiology. 2009;297(1):H417-H424. DOI:10.1152/ajpheart.01130.2008.

[32] Tewari K, Simard JM. Sodium nitroprusside and cGMP decrease Ca 2+ channel availability in basilar artery smooth muscle cells. Pflügers Archiv. 1996;433(3):304-311. DOI:10.1007/ s004240050281.

[33] Raeymaekers L, Hofmann F, Casteels R. Cyclic GMP-dependent protein kinase phosphorylates phospholamban in isolated sarcoplasmic reticulum from cardiac and smooth muscle. Biochemical Journal. 1988;252 (1):269-273. DOI:10.1042/bj2520269.

[34] Karczewski P, Kelm M, Hartmann M, Schrader J. Role of phospholamban in NO/EDRF-induced relaxation in rat aorta. Life sciences. 1992;51(15):1205-1210. DOI:10.1016/ 0024-3205(92)90357-u.

[35] Gustavsson M, Verardi R, Mullen DG, Mote KR, Traaseth NJ, Gopinath T, et al. Allosteric regulation of SERCA by phosphorylation-mediated conformational shift of phospholamban. Proceedings of the National Academy of Sciences. 2013;110(43):17338-17343. DOI:10.1073/pnas.1303006110.

[36] Murthy K, Severi C, Grider J, Makhlouf G. Inhibition of IP3 and IP3-dependent Ca2+ mobilization by cyclic nucleotides in isolated gastric muscle cells. American Journal of Physiology-Gastrointestinal and Liver Physiology. 1993;264(5):G967-G974. DOI:10.1152/ ajpgi.1993.264.5.g967.

[37] Furukawa Kl, Ohshima N, Tawada-Iwata Y, Shigekawa M. Cyclic GMP stimulates Na+/Ca2+ exchange in vascular smooth muscle cells in primary culture. Journal of Biological Chemistry. 1991;266(19):12337-12341. DOI:10.1016/ s0021-9258(18)98901-5.

[38] Vrolix M, Raeymaekers L, Wuytack F, Hofmann F, Casteels R. Cyclic GMP-dependent protein kinase stimulates the plasmalemmal Ca2+ pump of smooth muscle via phosphorylation of phosphatidylinositol. Biochemical Journal. 1988;255(3):855-863. DOI: 10.1042/bj2550855.

[39] Furukawa K, Tawada Y, Shigekawa M. Regulation of the plasma membrane Ca2+ pump by cyclic nucleotides in cultured vascular smooth muscle cells. Journal of Biological Chemistry. 1988;263(17):8058-8065. DOI:10.1016/s0021-9258(18)68441-8.

[40] Yoshida Y, Sun H-T, Cai J-Q, Imai S. Cyclic GMP-dependent protein kinase stimulates the plasma membrane Ca2+ pump ATPase of vascular smooth muscle via phosphorylation of a 240-kDa protein. Journal of Biological Chemistry. 1991;266(29):19819-19825. DOI:10.1016/s0021-9258(18)55065-1.

[41] Manoury B, Idres S, Leblais V, Fischmeister R. Ion channels as effectors of cyclic nucleotide pathways: Functional relevance for arterial tone

regulation. Pharmacology & therapeutics. 2020;209:107499. DOI: 10.1016/j.pharmthera.2020.107499.

[42] Schubert R, Nelson MT. Protein kinases: tuners of the BKCa channel in smooth muscle. Trends in pharmacological sciences. 2001;22(10): 505-512. DOI:10.1016/s0165-6147(00) 01775-2.

[43] Alioua A, Tanaka Y, Wallner M, Hofmann F, Ruth P, Meera P, et al. The large conductance, voltage-dependent, and calcium-sensitive K+ channel, Hslo, is a target of cGMP-dependent protein kinase phosphorylation in vivo. Journal of Biological Chemistry. 1998;273(49): 32950-32956. DOI:10.1074/ jbc.273.49.32950.

[44] Zhou X-B, Ruth P, Schlossmann J, Hofmann F, Korth M. Protein phosphatase 2A is essential for the activation of Ca2+-activated K+ currents by cGMP-dependent protein kinase in tracheal smooth muscle and Chinese hamster ovary cells. Journal of Biological Chemistry. 1996;271(33):19760-19767. DOI:10.1074/jbc.271.33.19760.

[45] Fellner SK, Arendshorst WJ. Complex interactions of NO/cGMP/ PKG systems on Ca2+ signaling in afferent arteriolar vascular smooth muscle. American Journal of Physiology-Heart and Circulatory Physiology. 2010;298(1):H144-H151. DOI:10.1152/ajpheart.00485.2009.

[46] Sausbier M, Arntz C, Bucurenciu I, Zhao H, Zhou X-B, Sausbier U, et al. Elevated blood pressure linked to primary hyperaldosteronism and impaired vasodilation in BK channel–deficient mice. Circulation. 2005;112(1): 60-68. DOI:10.1161/01. cir.0000156448.74296.fe.

[47] Matchkov VV, Aalkjaer C, Nilsson H. A cyclic GMP–dependent calcium-activated chloride current in smooth-muscle cells from rat mesenteric resistance arteries. Journal of General Physiology. 2004;123(2): 121-134. DOI:10.1085/jgp.200308972.

[48] Tamaoki J, Tagaya E, Nishimura K, Isono K, Nagai A. Role of Na+-K+ ATPase in cyclic GMP-mediated relaxation of canine pulmonary artery smooth muscle cells. British journal of pharmacology. 1997;122(1):112-116. DOI:10.1038/sj.bjp.0701351.

[49] O'Donnell ME, Owen N. Role of cyclic GMP in atrial natriuretic factor stimulation of Na+, K+, Cl-cotransport in vascular smooth muscle cells. Journal of Biological Chemistry. 1986;261(33): 15461-15466. DOI:10.1016/s0021-9258 (18)66734-1.

[50] Jacobsen JCB, Aalkjær C, Nilsson H, Matchkov VV, Freiberg J, Holstein-Rathlou N-H. Activation of a cGMP-sensitive calcium-dependent chloride channel may cause transition from calcium waves to whole cell oscillations in smooth muscle cells. American Journal of Physiology-Heart and Circulatory Physiology. 2007;293(1):H215-H228. DOI:10.1152/ajpheart.00726.2006.

[51] Kapela A, Bezerianos A, Tsoukias NM. A mathematical model of Ca2+ dynamics in rat mesenteric smooth muscle cell: agonist and NO stimulation. Journal of theoretical biology. 2008;253(2):238-260. DOI: 10.1016/j.jtbi.2008.03.004.

[52] Kiss A, Erdődi F, Lontay B. Myosin phosphatase: Unexpected functions of a long-known enzyme. Biochimica et Biophysica Acta (BBA)-Molecular Cell Research. 2019;1866(1):2-15. DOI: 10.1016/j.bbamcr.2018.07.023.

[53] Kimura K, Ito M, Amano M, Chihara K, Fukata Y, Nakafuku M, et al. Regulation of myosin phosphatase by Rho and Rho-associated kinase (Rho-kinase). Science. 1996;273(5272): 245-248. DOI:10.1126/ science.273.5272.245.

[54] Wooldridge AA, MacDonald JA, Erdodi F, Ma C, Borman MA, Hartshorne DJ, et al. Smooth muscle phosphatase is regulated in vivo by exclusion of phosphorylation of threonine 696 of MYPT1 by phosphorylation of Serine 695 in response to cyclic nucleotides. Journal of Biological Chemistry. 2004;279(33): 34496-34504. DOI:10.1074/jbc.m405957200.

[55] Gao Y, Portugal AD, Negash S, Zhou W, Longo LD, Usha Raj J. Role of Rho kinases in PKG-mediated relaxation of pulmonary arteries of fetal lambs exposed to chronic high altitude hypoxia. American Journal of Physiology-Lung Cellular and Molecular Physiology. 2007;292(3):L678-L684. DOI:10.1152/ajplung.00178.2006.

[56] Khromov A, Choudhury N, Stevenson AS, Somlyo AV, Eto M. Phosphorylation-dependent autoinhibition of myosin light chain phosphatase accounts for Ca2+ sensitization force of smooth muscle contraction. Journal of Biological Chemistry. 2009;284(32):21569-21579. DOI:10.1074/jbc.m109.019729.

[57] Terrak M, Kerff F, Langsetmo K, Tao T, Dominguez R. Structural basis of protein phosphatase 1 regulation. Nature. 2004;429(6993):780-784. DOI: 10.1038/nature02582.

[58] Grassie ME, Sutherland C, Ulke-Lemée A, Chappellaz M, Kiss E, Walsh MP, et al. Cross-talk between Rho-associated kinase and cyclic nucleotide-dependent kinase signaling pathways in the regulation of smooth muscle myosin light chain phosphatase. Journal of Biological Chemistry. 2012; 287(43):36356-36369. DOI:10.1074/jbc.m112.398479.

[59] Lubomirov L, Papadopoulos S, Filipova D, Baransi S, Todorović D, Lake P, et al. The involvement of phosphorylation of myosin phosphatase targeting subunit 1 (MYPT 1) and MYPT 1 isoform expression in NO/cGMP mediated differential vasoregulation of cerebral arteries compared to systemic arteries. Acta Physiologica. 2018;224(1):e13079. DOI: 10.1111/apha.13079.

[60] Eto M. Regulation of cellular protein phosphatase-1 (PP1) by phosphorylation of the CPI-17 family, C-kinase-activated PP1 inhibitors. Journal of Biological Chemistry. 2009; 284(51):35273-35277. DOI:10.1074/jbc.r109.059972.

[61] Smolenski A, Lohmann SM, Bertoglio J, Chardin P, Sauzeau V, Le Jeune H, et al. Cyclic GMP-dependent protein kinase signaling pathway inhibits RhoA-induced Ca2+ sensitization of contraction in vascular smooth muscle. Journal of Biological Chemistry. 2000;275(28):21722-21729. DOI:10.1074/jbc.m000753200.

[62] Roux E, Mbikou P, Fajmut A. Role of protein kinase network in excitation-contraction coupling in smooth muscle cell. Protein Kinases. 2012:287-320. DOI: 10.5772/37805.

[63] Butler T, Paul J, Europe-Finner N, Smith R, Chan E-C. Role of serine-threonine phosphoprotein phosphatases in smooth muscle contractility. American Journal of Physiology-Cell Physiology. 2013;304(6):C485-C504. DOI:10.1152/ajpcell.00161.2012.

[64] Mbikou P, Fajmut A, Brumen M, Roux E. Contribution of Rho kinase to the early phase of the calcium–contraction coupling in airway smooth muscle. Experimental physiology. 2011; 96(2):240-258. DOI:10.1113/expphysiol.2010.054635.

[65] Wu X, Haystead TA, Nakamoto RK, Somlyo AV, Somlyo AP. Acceleration of myosin light chain dephosphorylation and relaxation of smooth muscle by telokin: synergism with cyclic

nucleotide-activated kinase. Journal of Biological Chemistry. 1998;273(18): 11362-11369. DOI:10.1074/jbc.273.18.11362.

[66] Khromov AS, Momotani K, Jin L, Artamonov MV, Shannon J, Eto M, et al. Molecular mechanism of telokin-mediated disinhibition of myosin light chain phosphatase and cAMP/cGMP-induced relaxation of gastrointestinal smooth muscle. Journal of Biological Chemistry. 2012;287(25):20975-20985. DOI:10.1074/jbc.m112.341479.

[67] Yang J, Clark JW, Bryan RM, Robertson CS. Mathematical modeling of the nitric oxide/cGMP pathway in the vascular smooth muscle cell. American Journal of Physiology-Heart and Circulatory Physiology. 2005;289(2): H886-H897. DOI:10.1152/ajpheart.00216.2004.

[68] Yang J, Clark Jr JW, Bryan RM, Robertson C. The myogenic response in isolated rat cerebrovascular arteries: smooth muscle cell model. Medical engineering & physics. 2003;25(8): 691-709. DOI:10.1016/s1350-4533(03)00100-0.

[69] Zhou X-B, Arntz C, Kamm S, Motejlek K, Sausbier U, Wang G-X, et al. A molecular switch for specific stimulation of the BKCa channel by cGMP and cAMP kinase. Journal of Biological Chemistry. 2001;276(46): 43239-43245. DOI:10.1074/jbc.m104202200.

[70] Mistry D, Garland C. Nitric oxide (NO)-induced activation of large conductance Ca2+-dependent K+ channels (BKCa) in smooth muscle cells isolated from the rat mesenteric artery. British journal of pharmacology. 1998; 124(6):1131-1140. DOI:10.1038/sj.bjp.0701940.

[71] Lee MR, Li L, Kitazawa T. Cyclic GMP causes Ca2+ desensitization in vascular smooth muscle by activating the myosin light chain phosphatase. Journal of Biological Chemistry. 1997; 272(8):5063-5068. DOI:10.1074/jbc.272.8.5063.

[72] Stockand JD, Sansom SC. Mechanism of activation by cGMP-dependent protein kinase of large Ca (2+)-activated K+ channels in mesangial cells. American Journal of Physiology-Cell Physiology. 1996;271(5):C1669-C1677. DOI:10.1152/ajpcell.1996.271.5.c1669.

[73] Large WA, Wang Q. Characteristics and physiological role of the Ca (2+)-activated Cl-conductance in smooth muscle. American Journal of Physiology-Cell Physiology. 1996;271 (2):C435-C454. DOI:10.1152/ajpcell.1996.271.2.c435.

[74] Jacobsen JCB, Aalkjær C, Nilsson H, Matchkov VV, Freiberg J, Holstein-Rathlou N-H. A model of smooth muscle cell synchronization in the arterial wall. American Journal of Physiology-Heart and Circulatory Physiology. 2007;293 (1):H229-H237. DOI:10.1152/ajpheart.00727.2006.

[75] Di Francesco D, Noble D. A model of cardiac electrical activity incorporating ionic pumps and concentration changes. Philosophical Transactions of the Royal Society of London B, Biological Sciences. 1985;307 (1133):353-398. DOI:10.1098/rstb.1985.0001.

[76] Fotis H, Tatjanenko LV, Vasilets LA. Phosphorylation of the α-subunits of the Na+/K+-ATPase from mammalian kidneys and Xenopus oocytes by cGMP-dependent protein kinase results in stimulation of ATPase activity. European journal of biochemistry. 1999; 260(3):904-910. DOI:10.1046/j.1432-1327.1999.00237.x.

[77] Strieter J, Stephenson JL, Palmer LG, Weinstein AM. Volume-activated chloride permeability can

mediate cell volume regulation in a mathematical model of a tight epithelium. The Journal of general physiology. 1990;96(2):319-344. DOI: 10.1085/jgp.96.2.319.

[78] Lalli MJ, Shimizu S, Sutliff RL, Kranias EG, Paul RJ. [Ca2+] ihomeostasis and cyclic nucleotide relaxation in aorta of phospholamban-deficient mice. American Journal of Physiology-Heart and Circulatory Physiology. 1999;277(3):H963-H970. DOI:10.1152/ajpheart.1999.277.3.h963.

[79] Parthimos D, Edwards DH, Griffith T. Minimal model of arterial chaos generated by coupled intracellular and membrane Ca2+ oscillators. American Journal of Physiology-Heart and Circulatory Physiology. 1999;277 (3):H1119-H1144. DOI:10.1152/ ajpheart.1999.277.3.h1119.

[80] Imtiaz MS, Smith DW, van Helden DF. A theoretical model of slow wave regulation using voltage-dependent synthesis of inositol 1, 4, 5-trisphosphate. Biophysical journal. 2002;83(4):1877-1890. DOI:10.1016/ s0006-3495(02)73952-0.

[81] Fajmut A, Brumen M. MLC-kinase/ phosphatase control of Ca2+ signal transduction in airway smooth muscles. Journal of theoretical biology. 2008;252 (3):474-481. DOI:10.1016/j. jtbi.2007.10.005.

[82] Mbikou P, Fajmut A, Brumen M, Roux E. Theoretical and experimental investigation of calcium-contraction coupling in airway smooth muscle. Cell biochemistry and biophysics. 2006;46 (3):233-251. DOI:10.1385/cbb:46:3:233.

[83] Fajmut A, Dobovišek A, Brumen M. Mathematical modeling of the relation between myosin phosphorylation and stress development in smooth muscles. Journal of chemical information and modeling. 2005;45(6):1610-1615. DOI: 10.1021/ci050178a.

[84] Fajmut A, Brumen M, Schuster S. Theoretical model of the interactions between Ca2+, calmodulin and myosin light chain kinase. FEBS letters. 2005; 579(20):4361-4366. DOI:10.1016/j. febslet.2005.06.076.

[85] Kapela A, Nagaraja S, Tsoukias NM. A mathematical model of vasoreactivity in rat mesenteric arterioles. II. Conducted vasoreactivity. American Journal of Physiology-Heart and Circulatory Physiology. 2010;298(1): H52-H65. DOI:10.1152/ ajpheart.00546.2009.

[86] Koenigsberger M, Sauser R, Meister J-J. Emergent properties of electrically coupled smooth muscle cells. Bulletin of mathematical biology. 2005; 67(6):1253-1272. DOI:10.1016/j. bulm.2005.02.001.

[87] Garmaroudi FS, Handy DE, Liu Y-Y, Loscalzo J. Systems Pharmacology and Rational Polypharmacy: Nitric Oxide– Cyclic GMP Signaling Pathway as an Illustrative Example and Derivation of the General Case. PLoS computational biology. 2016;12(3): e1004822. DOI:10.1371/journal. pcbi.1004822.

[88] Koo A, Nordsletten D, Umeton R, Yankama B, Ayyadurai S, García-Cardeña G, et al. In silico modeling of shear-stress-induced nitric oxide production in endothelial cells through systems biology. Biophysical journal. 2013;104(10):2295-2306. DOI:10.1016/j. bpj.2013.03.052.

[89] Sriram K, Laughlin JG, Rangamani P, Tartakovsky DM. Shear-induced nitric oxide production by endothelial cells. Biophysical journal. 2016;111(1):208-221. DOI:10.1016/j. bpj.2016.05.034.

[90] Comerford A, Plank M, David T. Endothelial nitric oxide synthase and calcium production in arterial geometries: an integrated fluid

mechanics/cell model. Journal of biomechanical engineering. 2008;130 (1). DOI:10.1115/1.2838026.

[91] Gosak M, Markovič R, Dolenšek J, Rupnik MS, Marhl M, Stožer A, et al. Network science of biological systems at different scales: A review. Physics of life reviews. 2018;24:118-135. DOI:10.1016/ j.plrev.2017.11.003.